AN ABSTRACT OF THE THESIS OF

Bahador Rastegar for the degree of Master of Science in Electrical & Computer Engineering presented on April 3, 1986.

Title: Surface Recombination Velocity and Bulk Lifetime in GaAs and InP.

Redacted for Privacy

Abstract approved: ______________________
Dr. John F. Wager

An analytical expression is derived which allows the bulk minority carrier recombination lifetime, τ, and the surface recombination velocity, S, to be extracted from a single noncontact photoconductivity decay (PCD) measurement. This analytical expression is rather complex, but can be reduced to a first order approximation. The first order approximation is different, however, for GaAs and InP than for Si, because of the large optical absorption coefficients and small lifetimes associated with III-V compound semiconductors. A comparison of the computer simulation of the more complex expression and the first order approximation reveals that the first order approximation model is accurate and is equally valid for both n-type and p-type materials.

Surface Recombination Velocity and Bulk Lifetime in GaAs and InP

by

Bahador Rastegar

A THESIS

submitted to

Oregon State University

in partial fulfillment of
the requirements for the
degree of

Master of Science

Completed: April 3, 1986

Commencement: June 1986

APPROVED:

Redacted for Privacy

Assistant Professor of Electrical & Computer Engineering

Redacted for Privacy

Head of Department of Electrical & Computer Engineering

Redacted for Privacy

Dean of Graduate School

Date thesis is presented April 3, 1986

Typed by Laurie Campbell for Bahador Rastegar

ACKNOWLEDGEMENT

My special thanks and sincere gratitude to my advisor, Dr. John F. Wager, for his excellent guidance, advice, and encouragement throughout the course of this thesis. He has been a major source of motivation in my graduate program.

I wish to extend my thanks to Dr. L. Forbes and Professor L.C. Jensen for being on my graduate committee and providing their suggestions. Thanks also to Dr. J.A. VanVechten for reviewing my thesis.

TABLE OF CONTENTS

Chapter 1 - **INTRODUCTION** 1

Chapter 2 - **THEORY OF SURFACE RECOMBINATION VELOCITY** 4

2.1 Surface Recombination 4
2.2 Steady-State Distribution of Excess Carriers 8

Chapter 3 - **THE METHOD OF ANALYSIS** 13

3.1 The Photoconductivity Technique 13
3.2 The Analytical Model 16
3.2.1 The Excess Carrier Concentration Equation 16
3.2.2 The Time-Dependent PCD Signal 20
3.3 The Constant Terms 21

Chapter 4 - **SURFACE RECOMBINATION VELOCITY AND PCD SIGNAL** 26

4.1 Analysis and Simulation for GaAs and InP 27
4.2 The First Order Approximation 31
4.2.1 Silicon 34
4.2.2 GaAs and InP 39

Chapter 5. **CONCLUSIONS AND FUTURE WORK** 46

BIBLIOGRAPHY 50

Appendix A - **THE CONTINUITY EQUATION** 52

Appendix B - **DERIVATION OF THE TIME-DEPENDENT PCD SIGNAL** 63

Appendix C - C.1 **NEGATIVE RATIO OF THE SLOPES OF THE PCD SIGNAL** 69
C.2 **THE COMPUTER SIMULATION** 73
C.3 **THE FIRST ORDER APPROXIMATION** 78

LIST OF FIGURES

Figure		Page
2.1	(a) Electron-hole pair generation by light, $h\nu > E_g$; (b) distribution of excess minority carriers.	6
2.2	A p-type semiconductor sample under illumination: (a) top view; (b) cross-sectional view.	9
2.3	Excess minority carrier distribution.	10
2.4	Illustration of steady-state excess minority carriers versus distance.	12
3.1	Apparatus for PCD measurement.	15
3.2	Creation of excess charge carriers: (a) photoexcitation; (b) side view of the sample.	17
3.3	Excess carrier distribution function versus distance.	23
3.4	Integral of an arbitrary function, f(x), from a to b.	25
4.1	Photoconductivity signal before and after the laser pulse.	27
4.2	A comparison of the actual surface recombination velocity for various values of the excess minority carrier lifetime [Eq. (4.5)].	29
4.3	A comparison of the actual surface recombination velocity for various values of the excess minority carrier lifetime [Eq. (4.5)].	30
4.4	Surface recombination velocity, S, for various values of Alpha.	32
4.5	Negative ratio of the photoconductivity signal (decay/increase) versus surface recombination velocity for various values of Alpha.	33
4.6	A plot of the first order approximation of m versus the surface recombination velocity.	35

4.7 Actual variation of the negative ratio of the slopes of the PCD signal versus S for various values of bulk lifetime. 36

4.8 A comparison between the actual and the approximate model. 37

4.9 A plot of the first order approximation model against the actual variation of the surface recombination velocity, S. 42

4.10 A plot of the first order approximation model against the actual variation of the surface recombination velocity, S. 44

LIST OF TABLES

Table		Page
1	Absorption Coefficient of InP for Various Values of Wavelength	26
2	Absorption Coefficient of GaAs for Various Values of Wavelength	26

SURFACE RECOMBINATION VELOCITY AND

BULK LIFETIME IN GaAs AND InP

CHAPTER 1

INTRODUCTION

Surface recombination is the result of an increased density of traps near the surface which enhances the recombination of electrons and holes. This causes a net current flow toward the surface of the semiconductor. Under some conditions, the rate of recombination at the surface may be even greater than that of the bulk recombination rate. Therefore, special care must be taken to ensure that the surface recombination rate is not intolerably high. Surface recombination in optical devices tends to be undesirable because, as a result of recombination at the surface, carriers will be removed from the essential and desirable radiative recombination path [1]. For example, the performance of photoconductive infrared detectors can be severely degraded because of surface leakage currents associated with a large surface recombination velocity.

A nondestructive method for simultaneous determination of the bulk recombination lifetime and surface recombination velocity in silicon has been developed by Eranen and Blomberg [2]. This method employs the photoconduc-

tivity decay (PCD) technique in which the decay of the total excess carrier charge is monitored as a function of time. Their method is based on a mathematical analysis of the transient decay of excess carriers as described by Tyagi et al. [3]. Eranen and Blomberg's method involves a complex relationship between the ratio of the slopes of the PCD signal and surface recombination velocity in silicon which is described in Chapter 3.

The primary purpose of this thesis is to extend the applicability of the PCD method [2] to III-V compounds, particularly GaAs and InP. One of the most significant results presented in this thesis is the development of a first order analytical approximation for GaAs and InP which can be used for the determination of the surface recombination velocity and bulk recombination lifetime. This first order approximation for GaAs and InP is different, however, than that arrived at for silicon by Eranen and Blomberg. Thus, it is shown that a straightforward application of their method, which is developed for the determination of surface recombination velocity and bulk recombination lifetime in silicon, to III-V semiconductor compounds would lead to erroneous results.

The theory of surface recombination velocity is covered in Chapter 2. Subsequently a detailed description of the PCD technique and the analytical model for the determination of the surface recombination velocity and

recombination lifetime is presented in Chapter 3. Analysis of the surface recombination velocity as a function of the bulk lifetime and the optical absorption coefficient of GaAs and InP along with the computer simulation is described in Chapter 4.

CHAPTER 2

THEORY OF SURFACE RECOMBINATION VELOCITY

Unfortunately, the effect of the surfaces of a finite crystal is not solely to confine charge carriers to the interior of the sample. If this were the case, the boundary condition which the excess charge carrier distribution would have to satisfy at the sample surfaces would simply be that the electron and hole current must vanish at the surface. However, charge carriers may recombine at the surface. Therefore, the recombination of carriers at the surface must be taken into account by defining a surface recombination velocity, $S(cm \cdot s^{-1})$ which represents a net current flow toward the surface of the sample. In thermal equilibrium there is no net flux toward the surface and the carrier concentration at the surface does not change. This is because, in addition to recombination, thermal generation of electron-hole pairs takes place at the surface. So, in thermal equilibrium the generation rate precisely equals the rate at which carrier pairs recombine at the surface.

2.1 Surface Recombination

Surface recombination is one of the parameters that should be considered in the design of many devices. In general, the rate of return of the minority carrier dis-

tribution to equilibrium depends on the rate constant characterizing the recombination process. The purpose of this section is to provide the reader with a basic understanding of surface recombination velocity and its origin. Surface recombination occurs as the result of diffusion or drift of electrons and holes to the surface and recombination there. Consider the case [4] illustrated in Figure 2.1. An increase in the concentration of recombination centers located within a very thin layer near the surface will enhance the recombination rate near the surface. Therefore, the excess carrier density will be smaller there.

Carriers will recombine at the surface due to the flow of fluxes of carriers from the bulk of the semiconductor. In order to derive an equation for the surface recombination velocity it is necessary to find the total flux of carriers recombining at the surface layer,

$$F_{surface} = \sigma_n v_{th} C_s \, [n_p(0) - n_{po}] \qquad (2.1)$$

where

σ_n = capture cross section of the centers

v_{th} = thermal velocity of the carriers at room temperature

C_s = concentration of surface recombination centers per unit area

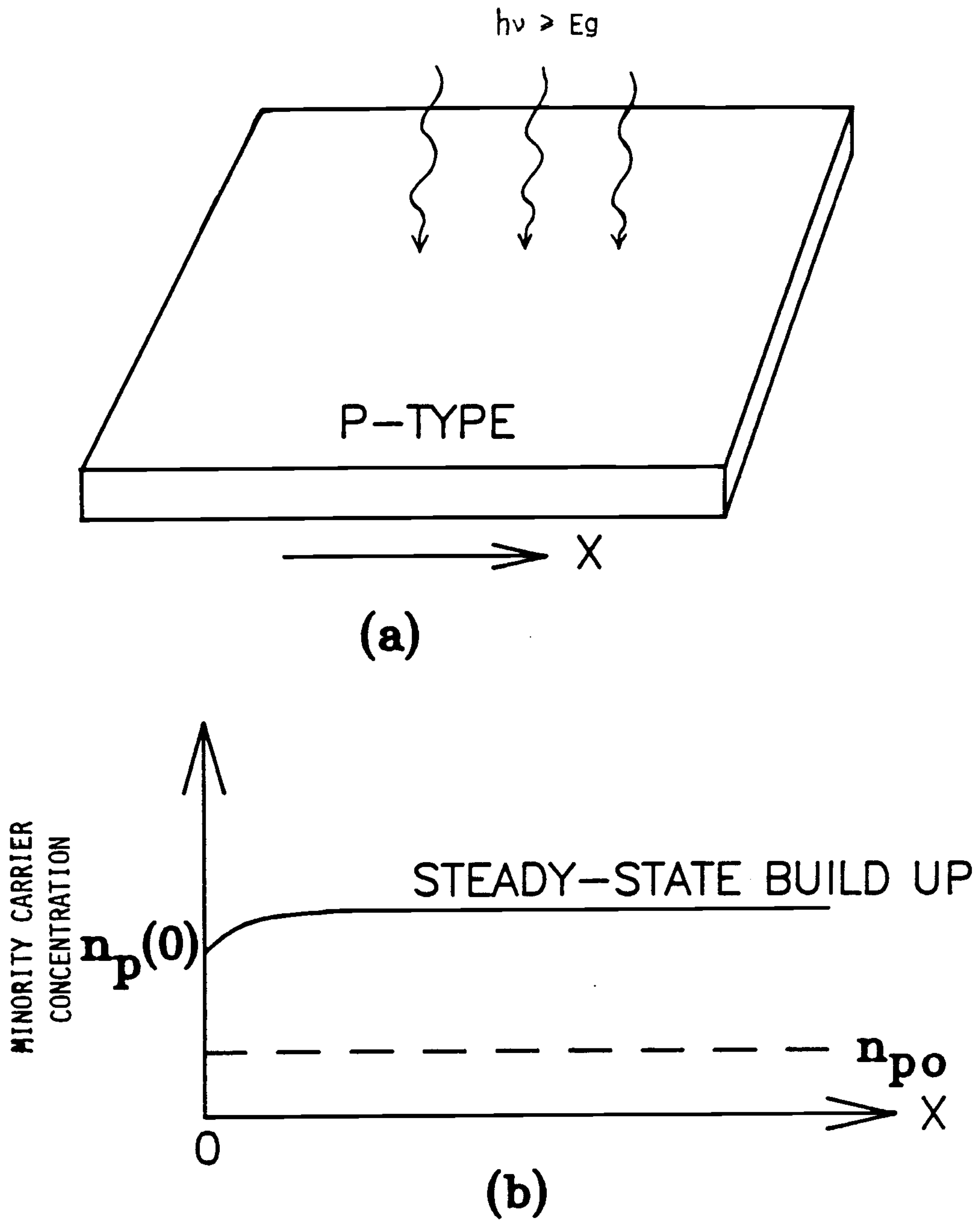

Figure 2.1. (a) Electron-hole pair generation by light, $h\nu \geq E_g$; (b) distribution of excess minority carriers.

$n_p(0)$ = excess minority carrier concentration at the surface

n_{po} = minority carrier concentration at equilibrium

The flux of minority carriers [5] to the surface is

$$D_n\left(\frac{\partial(\Delta n)}{\partial x}\right)\bigg|_{x=0} = F_{surface} \ . \tag{2.2}$$

This equation is a statement of the surface boundary condition which must be applied to the continuity equation. It can be written that

$$D_n\left(\frac{\partial(\Delta n)}{\partial x}\right)\bigg|_{x=0} = S \cdot (\Delta n)\bigg|_{surface} \tag{2.3}$$

where $\Delta n|_{surface} = n_p(0) - n_{po}$ and S is referred to as the surface recombination velocity (cm/s). Equation (2.3) simply states that the minority carriers that reach the surface recombine there. This may also be regarded as a definition for the surface recombination velocity. Thus, the surface recombination velocity is a proportionality constant which relates the recombination rate at the surface to the excess minority carrier density there.

From a comparison of Eqs. (2.1), (2.2), and (2.3) it is possible to show that

$$S = \sigma_n v_{th} C_s \ . \tag{2.4}$$

This relationship for surface recombination velocity may change in the case of charges existing at the surface [4]. Consequently, as the surface charge is varied, the surface recombination velocity will vary as well.

2.2 Steady-State Distribution of Excess Carriers

In this case the semiconductor sample is investigated at the front surface from which the excess carriers are injected (y-axis is taken parallel to the incident beam). The schematic diagram is illustrated in Figure 2.2.

Consider the case of a p-type semiconductor. Assume that the excess minority carrier concentration due to optical generation is within a very thin layer, ℓ, of the surface. Because of the concentration gradient, excess minority carriers tend to diffuse toward the bulk away from the surface as shown in Figure 2.3.

In steady-state it can be written that

$$\frac{\partial n_p}{\partial t} = 0 \tag{2.5}$$

and the minority carrier transport equation (assuming no generation) is given by

$$\frac{\partial n_p}{\partial t} = D_n \frac{d^2 n_p}{dy^2} - \frac{\Delta n}{\tau_n} = 0 \tag{2.6}$$

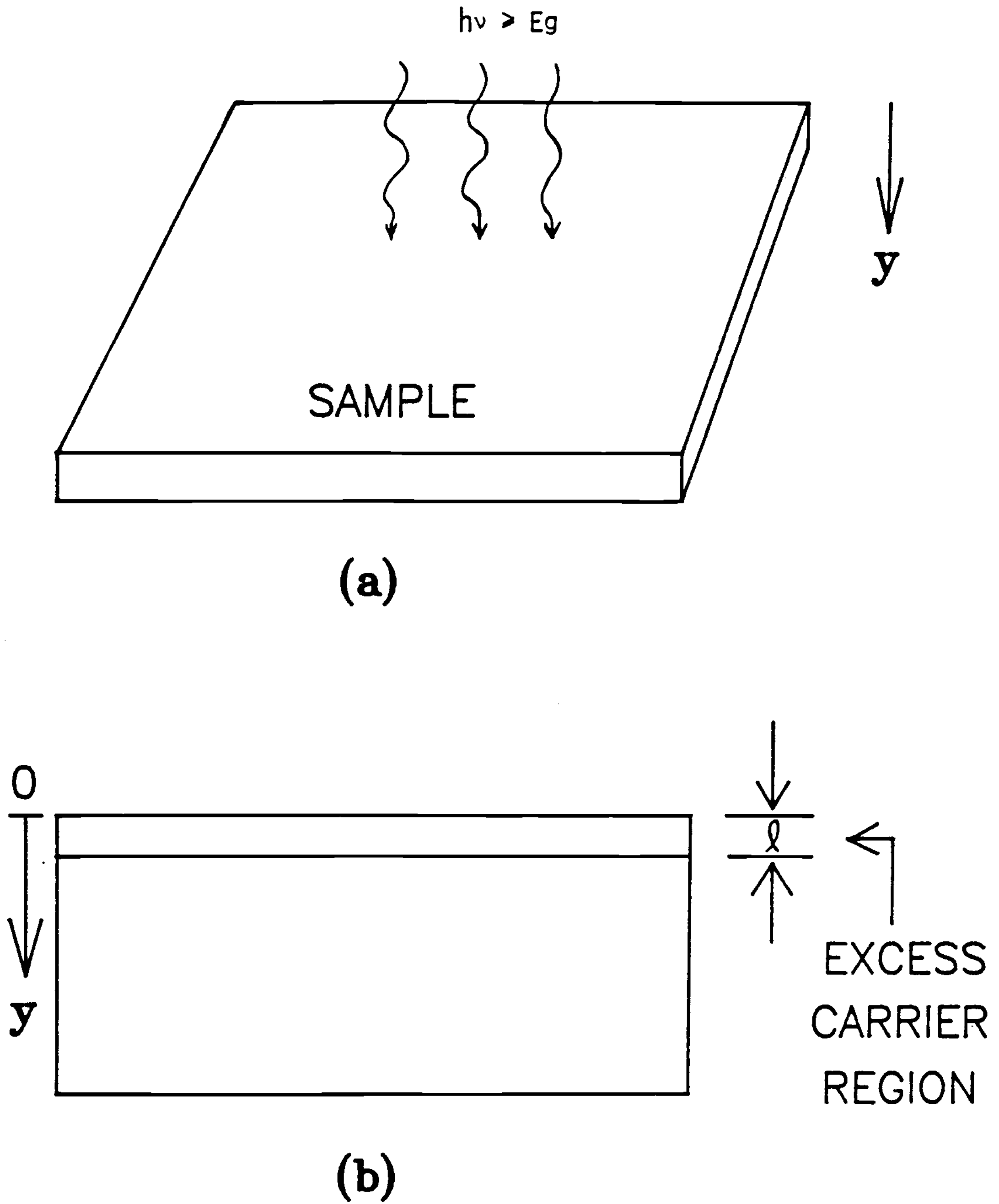

Figure 2.2. A p-type semiconductor sample under illumination: (a) top view; (b) cross sectional view.

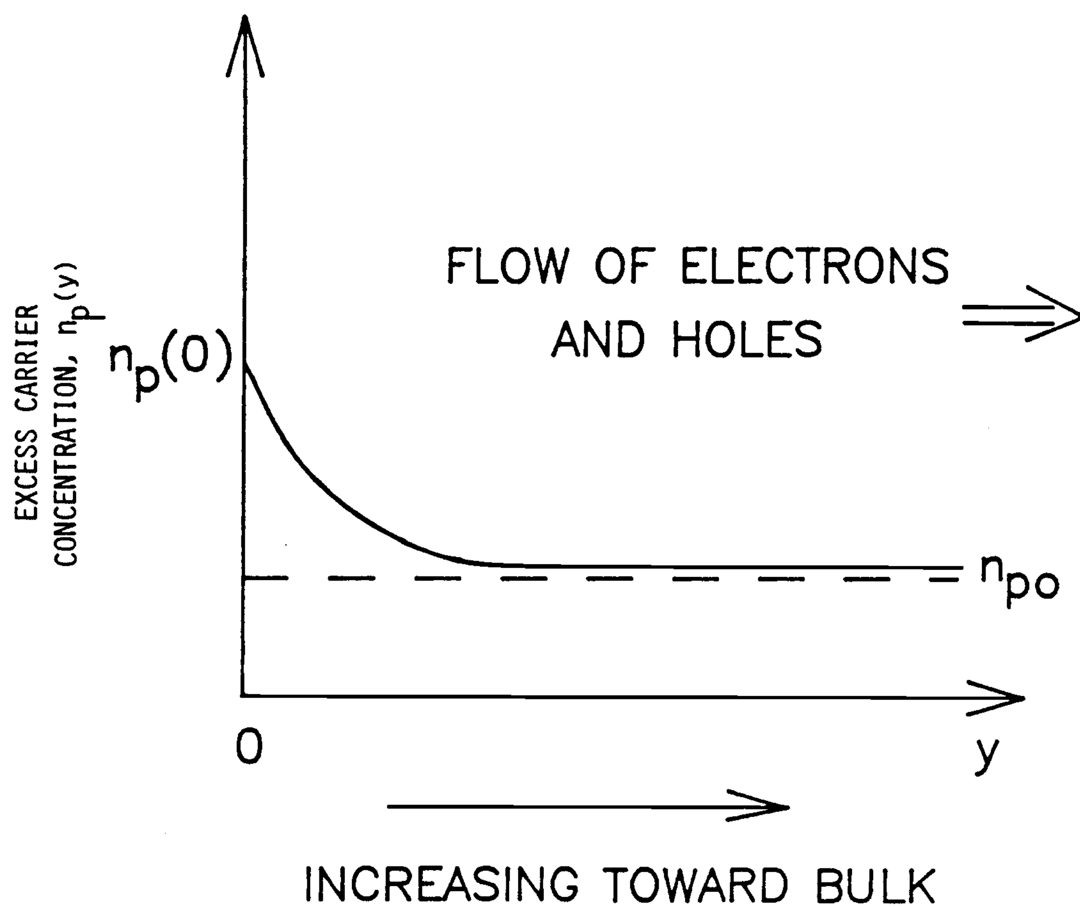

Figure 2.3. Excess minority carrier distribution.

where τ_n is the minority carrier lifetime. Boundary conditions are given as

$$n_p = \begin{cases} n_{po} \text{ at } y = \infty \text{ (Deep in the bulk)} \\ \\ \text{constant at } y = 0 \; (n_p(0)) \end{cases} \tag{2.7}$$

Then

$$\frac{d^2 n_p}{dy^2} - \frac{n_p}{D_n \tau_n} = \frac{n_{po}}{D_n \tau_n} \tag{2.8}$$

and the total solution [6] is

$$n_p(y) = A_1 e^{-y/L_n} + n_{po} \tag{2.9}$$

where $L_n = \sqrt{D_n \tau_n}$ is the diffusion length. Using the boundary conditions, the minority carrier distribution can be shown to be

$$n_p(y) = (n_p(0) - n_{po})\, e^{-y/L_n} + n_{po} \tag{2.10}$$

which gives the steady-state distribution of excess minority carriers as a function of distance.

Equation (2.10) is used in some analytical portions of Chapter 3. A plot of Eq. (2.10) as a function of dis-

tance is shown in Figure 2.4 for different values of L_n. It is important to note that as L_n decreases the decay of the minority carriers becomes sharper. In addition, since $L_n = (D_n\tau_n)^{1/2}$ the decay of minority carriers with respect to time is also faster with decreasing minority carrier lifetime.

This analysis will be useful for simplification of the analytical model for determination of surface recombination velocity presented in the next chapter.

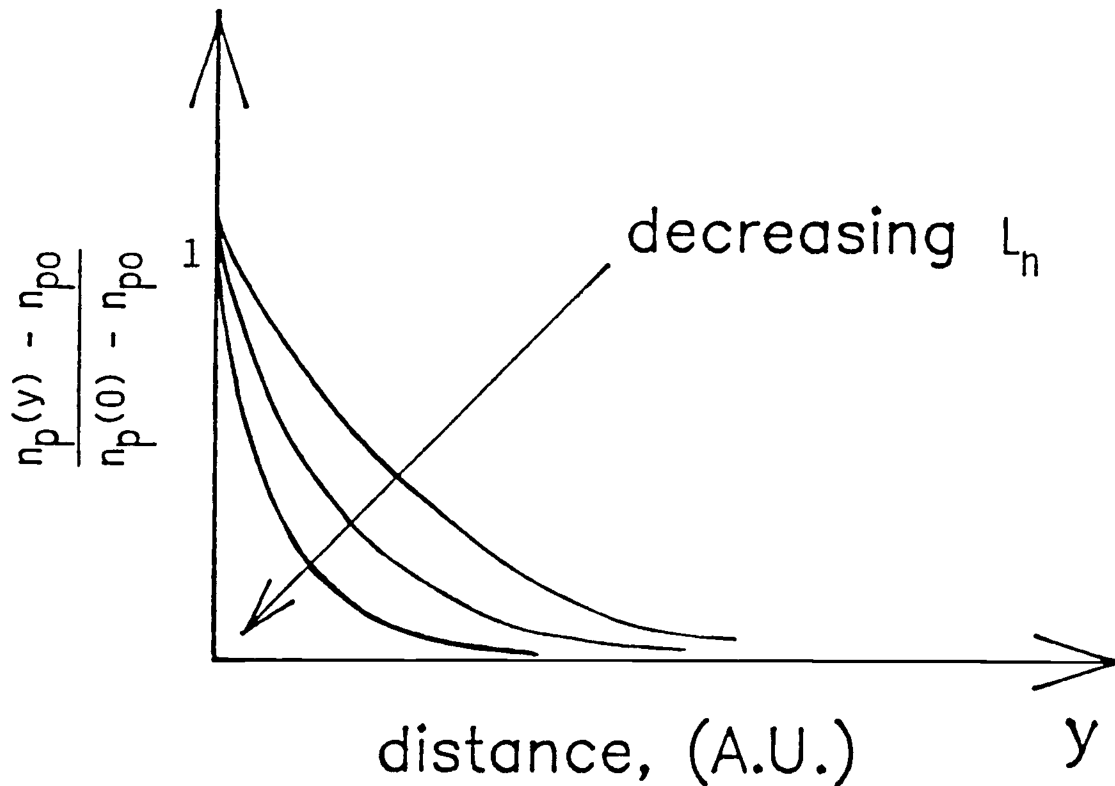

Figure 2.4. Illustration of steady-state excess minority carriers versus distance.

CHAPTER 3
THE METHOD OF ANALYSIS

When electrons are excited to higher energy levels in a solid they can return to equilibrium by means of recombination. Carrier pairs within a diffusion length of the surface of a semiconductor can recombine at the surface, resulting in surface recombination. In this chapter an extension of the mathematical analysis of the PCD method is presented which allows the determination of the surface recombination velocity and recombination lifetime in GaAs and InP. Although the analytical development is mathematically rather complicated, the results are reduced to a simple form which is fairly easy to use. As a result, the surface recombination velocity for InP or GaAs can be extracted from a first order approximation equation.

3.1 The Photoconductivity Technique

The photoconductivity decay (PCD) method employs a short laser pulse ($h\nu > E_g$) as a source to excite carriers near a thin surface layer with a thickness of the order of α^{-1}, where α is the optical absorption coefficient. The value of α^{-1} is chosen to be very small compared to the sample thickness. The PCD transient decay is monitored using a microwave or laser probe. The measurement

described by Eranen and Blomberg [2] utilized a 24-GHZ microwave power to probe the changes of the conductivity in the sample. A GaAs laser diode giving 100-ns pulses with 25-W optical power was used as the source laser. The reflected and sensitive microwave or laser signal which is detected as a function of time is the desired PCD transient. A simple schematic diagram illustrating the measurement apparatus is shown in Figure 3.1. The experimental parameter used to extract the surface recombination velocity and the bulk lifetime is denoted by the symbol m. This symbol is defined as the negative ratio of the slopes of the photoconductivity signal; that is,

$$m = - \frac{dp/dt|_{t > t_d}}{dp/dt|_{0 < t < t_d}} \qquad (3.1)$$

where $dp/dt|_{t > t_d}$ and $dp/dt|_{0 < t < t_d}$ are, respectively, the slopes of the PCD signal determined just after and before the laser pulse ends. t_d is the duration of laser pulse ($t_d << \tau$). When the laser source is on, electron-hole pairs are generated near the surface which in turn causes a momentary increase in the conductivity. The photo-generated excess carriers then recombine during the "OFF" time of the pulse.

One of the attractive features of this method is that there is no actual physical contact to the sample and that photoexcitation is easy to implement. Moreover, the

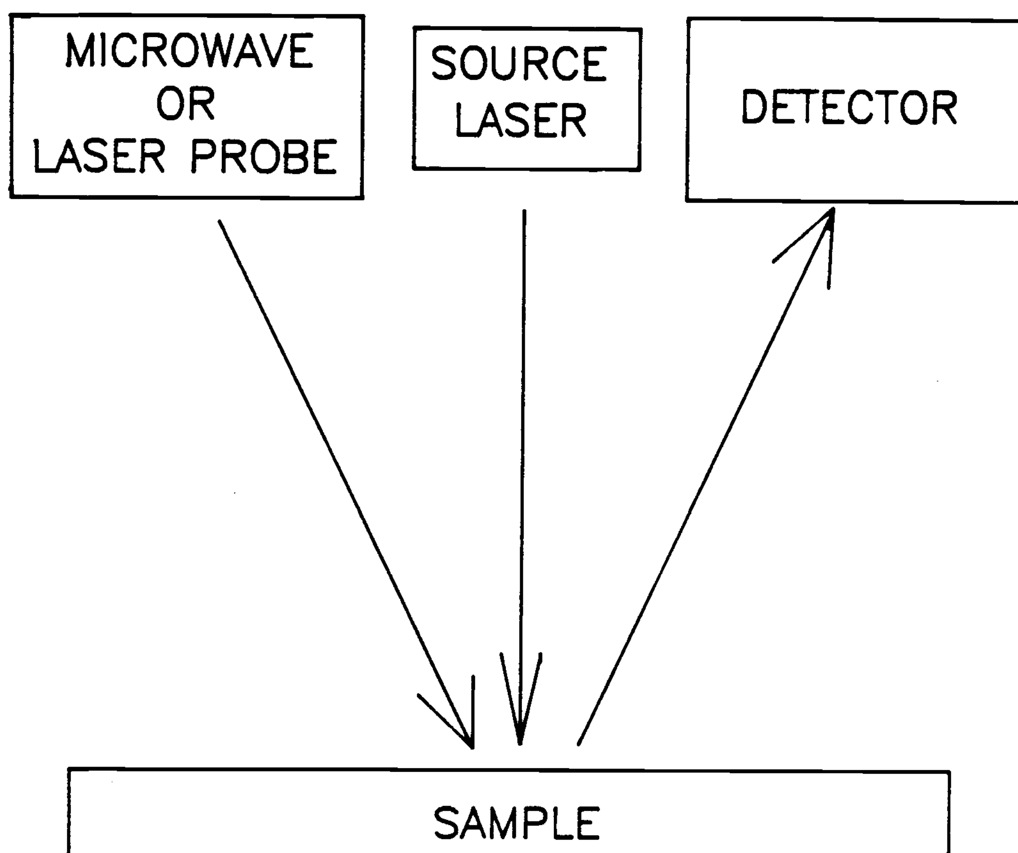

Figure 3.1. Apparatus for PCD measurement.

excess carrier lifetime and surface recombination velocity can be determined in a single PCD measurement.

3.2 The Analytical Model

In this section the time-dependent solution to the one-dimensional continuity equation for the excess minority carriers (assuming that the surface recombination is important only on the front surface in which the excess carriers are injected) is used to calculate the decay of the total excess carrier charge as a function of time for different values of the surface recombination velocity. This result is subsequently used to derive an analytical PCD expression for the determination of the surface recombination velocity.

3.2.1 The Excess Carrier Concentration Equation

Consider a uniform p-type semi-infinite semiconductor sample which is illuminated with an incident beam as shown in Figure 3.2. It is assumed that the sample has dimensions of x, y, z where the thickness, x is much less than the other dimensions y and z so that the surface recombination is important only on y-z plane. However, the thickness is at least a few multiples of the diffusion length, $L = (D\tau)^{1/2}$, or the effective diffusion length, $\ell \simeq \frac{1}{\alpha} + (Dt_d)^{1/2}$, whichever is a larger quantity. It is assumed that the illumination is perpendicular to the

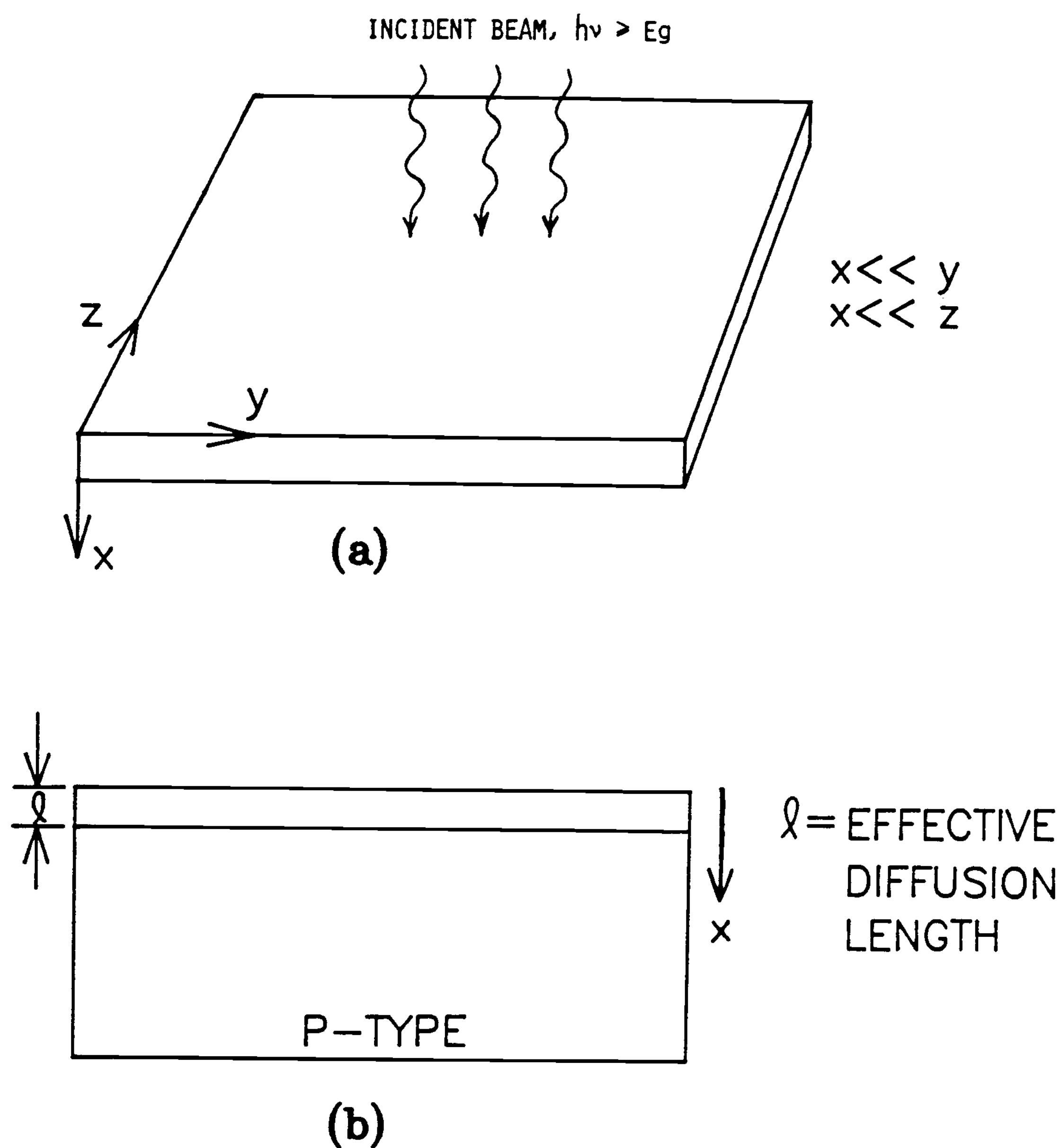

Figure 3.2. Creation of excess charge carriers: (a) photoexcitation; (b) side view of the sample.

surface along the x-axis and the excess carriers are generated uniformly near the surface by the light pulse and finally the injection level is low. From the minority carrier continuity equation,

$$\frac{1}{D}\frac{d(\Delta n)}{dt} = \frac{d^2(\Delta n)}{dx^2} - \frac{\Delta n}{D\tau} + \frac{C_g(x)}{D} \qquad (3.2)$$

where $C_g(x)$ is the excess carrier generation rate with the form

$$C_g(x) = c_o\ e^{-\alpha x}\ [1 - U(t - t_d)]\ . \qquad (3.3)$$

Here α is the absorption coefficient, t_d is the duration of laser pulse ($t_d << \tau$), and Δn and τ represent the excess minority carrier concentration and minority carrier lifetime, respectively. Finally, U(t) represents a unit step function.

Equation (3.2) may be solved using the following boundary conditions

$$D\left.\frac{d(\Delta n)}{dx}\right|_{x=0} = S \cdot \Delta n\ (0,t) \qquad (3.4)$$

which simply states that the minority carriers that reach the surface recombine there with an associated surface recombination velocity of S. Also,

$$\Delta n(x,t)\Big|_{t=0} = 0$$

$$\Delta n(x,t)\Big|_{x=\infty} = 0 \; . \qquad (3.5)$$

It can be shown [Appendix A] that the time domain solution of the excess carrier concentration, Eq. (3.2), is

$$N(x,t) = \begin{cases} C(x,t) & \text{if } t < t_d \\ C(x,t) - C[x,(t - t_d)] & \text{if } t > t_d \end{cases} \qquad (3.6)$$

where

$$C(x,t) = \mathbf{L}^{-1}[C_1(x,\mathbf{s})] + \mathbf{L}^{-1}[C_2(x,\mathbf{s})] \qquad (3.7)$$

Because of the complexity of Eq. (3.7), the exact expressions are shown in Appendix [A] for $\mathbf{L}^{-1}[C_1]$ and $\mathbf{L}^{-1}[C_2]$ in Eqs. (A.30) and (A.32), respectively.

A similar result has been reported by Tyagi et al. [3] in their study of surface recombination effects on the transient decay of excess carriers confined within a very thin layer near the surface. Note that the decrease in the excess minority carrier concentration near the surface due to surface recombination extends to a distance of the

order of a few times the diffusion length from the surface.

3.2.2 The Time-Dependent PCD Signal

In this section it is shown that it is possible to determine the surface recombination velocity and excess carrier lifetime in III-V compounds fairly accurately from the PCD measurement. In the previous section it was found that the laser pulse duration is chosen to be much less than τ which means that the excess carrier distribution will be within a thin layer on the order of the effective diffusion length (Figure 3.2). Having found the excess carrier concentration in Section 3.2.1, the time dependence of the PCD signal, P(t), for a short laser pulse duration can be obtained by integrating [Appendix B] the solution of the excess carrier per unit area [Eq. (A.33)]. This gives

$$P(t) = C(t)\ U(t) - C(t - t_d)\ U(t - t_d) \qquad (3.8)$$

where U is a unit step function and C(t) can be shown [Appendix B] to be

$$C(t) = \frac{c_o \tau L e^{-t/\tau}}{(D\tau\alpha^2 - 1)[(\frac{S^2\tau}{D}) - 1][(\frac{SL}{D}) - \alpha L]}$$

$$\cdot \{(D\tau\alpha^2 - \frac{S^2\tau}{D})(\frac{SL}{D}) \cdot e^{t/\tau} \operatorname{erfc}(\sqrt{\frac{t}{\tau}})$$

$$+ (\frac{S^2\tau}{D} - 1)\, e^{\alpha^2 L^2 t/\tau} \cdot (\frac{S}{\alpha D}) \operatorname{erfc}(\alpha L \sqrt{\frac{t}{\tau}})$$

$$- (D\tau\alpha^2 - 1)\, e^{(\frac{S^2 t}{D})} \operatorname{erfc}(\frac{SL}{D}\sqrt{\frac{t}{\tau}})\} + \text{CONST.} \qquad (3.9)$$

A similar result has also been reported by Eranen and Blomberg [2]. These authors asserted that the constant term in Eq. (3.9) is an unimportant term. However, the authors have provided no justification for disregarding this term. Additionally, it is not clear whether this term may be neglected for the case of GaAs and InP. This constant term is divided into several subterms which are studied in the following section.

3.3 The Constant Terms

Some of the constant subterms associated with Eq. (3.9) are indicated in Eqs. (B.7) and (B.8) [Appendix B]. Evaluation of Eq. (B.7) by computer reveals that the final contribution of these constant terms is very small and usually negligible. Although including these terms improves the accuracy of the analytical calculation slightly, the analytical formulation may become even more

complex and loses its simplicity and utility. The computer analysis has been carried out for Si, GaAs, and InP samples. As an example, for p-type InP with the following parameters; $T = 300°K$, $\mu_n = 4600\ cm^2/V\text{-}sec$ ($D_n = 120\ cm^2/s$), $\alpha = 5.4x10^4\ cm^{-1}$, $\tau_n = 1$ nanosecond, and $t_d = 0.1$ nanosecond. The final contribution of Eq. (B.7) is in the order of 10^{-6} which is negligible compared to the rest of the terms which are of the order of 10^{-3}.

Equation (B.8) may be written as

$$\frac{-L}{\sqrt{Dt\pi}} \int_0^{\ell} e^{-\left(\frac{x^2}{4Dt} + \frac{t}{\tau}\right)} dx = \frac{-Le^{-\frac{t}{\tau}}}{\sqrt{Dt\pi}} \int_0^{\ell} e^{\frac{-x^2}{4Dt}} dx \qquad (3.10)$$

Let $a = \frac{1}{4Dt}$, then Eq. (3.10) can be simplified to

$$\frac{-Le^{-\frac{t}{\tau}}}{\sqrt{Dt\pi}} \int_0^{\ell} e^{-ax^2} dx \qquad (3.11)$$

which is similar to the normal probability distribution function. Note that the general form of the distribution function using the Gaussian random variable [8] is

$$F_x(x) = \frac{1}{\sqrt{2\pi\sigma_x^2}} \int_{-\infty}^{x} e^{-(\xi - a_x)^2/2\sigma_x^2} d\xi . \qquad (3.12)$$

However, this integral has no known closed-form solution and must be evaluated by numerical methods. Remember that

in this case the distribution of excess carriers is confined to a very thin layer of the surface, ℓ, which is on the order of $1/\alpha$ and follows the normalized form of Eq. (3.12). The general behavior of this equation is indicated in Figure 3.3.

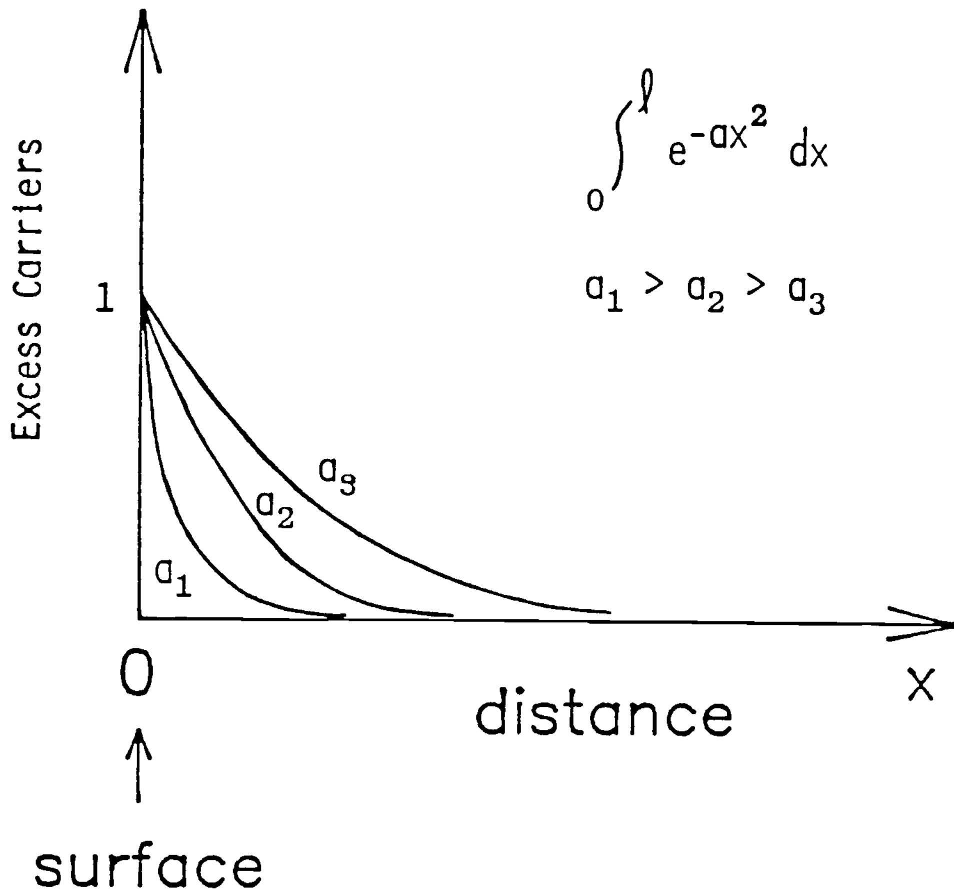

Figure 3.3. Excess carrier distribution function versus distance.

It turns out that the numerical value of Eq. (3.11) is negligible. This can be seen using the following property from integral calculus (see Figure 3.4),

$$\left| \int_a^b f(x)dx \right| < M(b - a) \ . \tag{3.13}$$

For example, for InP with $D_n = 120\ cm^2/s$ and $t_d = 0.1$ nanosecond, Eq. (3.11) can be reduced to

$$\int_o^{\ell} e^{-10^7 x^2}\, dx < \ell$$

which indicates that the initial decay is extremely fast especially when ℓ is on the order of $1/\alpha$.

Therefore, assuming that the absorption coefficient, α, is large and the pulse duration, t_d, is small ($t_d << \tau$) the terms in Eq. (B.8) can be neglected. A similar approach may be used to verify neglecting the rest of the constant subterms associated with Eq. (3.9). These constant subterms which are similar to Eqs. (B.7) and (B.8) can be found by performing the integrations indicated in Eqs. (B.1b), (B.1c), and (B.1d).

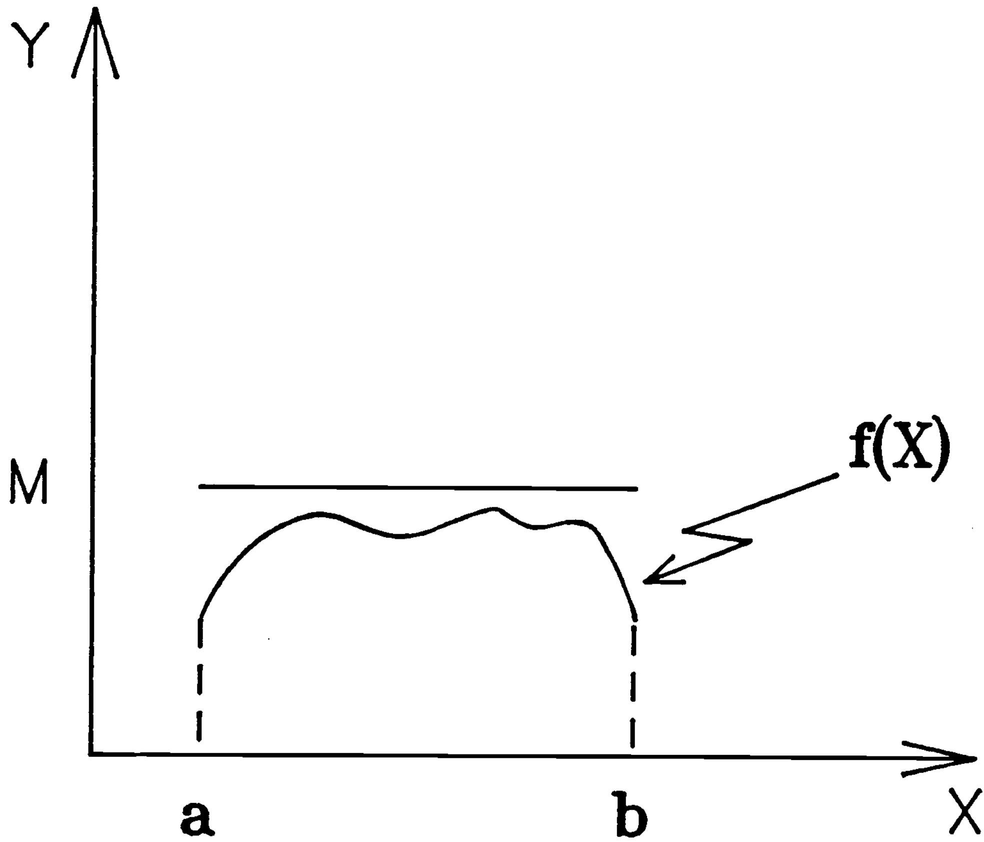

Figure 3.4. Integral of an arbitrary function, f(x), from a to b.

CHAPTER 4

SURFACE RECOMBINATION VELOCITY AND PCD SIGNAL

A derivation of a relationship between surface recombination velocity and the PCD signal is presented in this chapter. The values used for the absorption coefficient, α, for InP and GaAs are summarized [11,12,13,14] in Tables 1 and 2, respectively.

Table 1. Absorption Coefficient of InP for Various Values of Wavelength.

λ, Å	α, cm^{-1}	Photon Energy
6,328	56,000	He-Ne Laser
8,200	21,454	GaAs Laser
8,732	12,952	Arbitrary Wavelength
9,200	7,796	Cutoff Wavelength

Table 2. Absorption Coefficient of GaAs for Various Values of Wavelength.

λ, Å	α, cm^{-1}	Photon Energy
6,328	92,000	He-Ne Laser
8,200	9,685	GaAs Laser
8,732	4,576	Cutoff Wavelength

4.1 Analysis and Simulation for GaAs and InP

The goal of this analysis is to extract the surface recombination velocity and minority carrier lifetime from the experimentally determined PCD signal which is shown in Figure (4.1). This analysis is accomplished by first measuring the value of the negative ratio of the slopes (decay/increase) of the PCD signal [Figure (4.1)], m.

Thus, m is defined as

$$m = - \frac{\left.\frac{dP}{dt}\right|_{t > t_d}}{\left.\frac{dP}{dt}\right|_{0 < t < t_d}} . \tag{4.1}$$

Equation (4.1) can be reduced [Appendix C.1] to:

$$m = \frac{\left.\frac{dC}{dt}\right|_{t = 0}}{\left.\frac{dC}{dt}\right|_{t = t_d}} - 1 \tag{4.2}$$

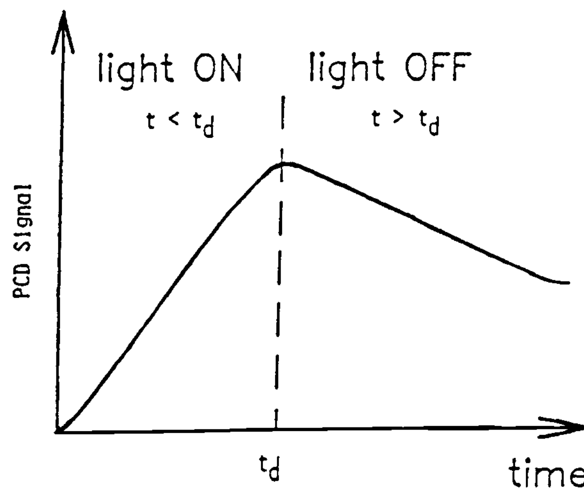

Figure 4.1. Photoconductivity signal before and after the laser pulse.

where $\frac{dC}{dt}$ is presented in Appendix [C.1], and

$$\left.\frac{dC}{dt}\right|_{t=0} = \frac{c_o L}{[(\frac{SL}{D}) - \alpha L]} \{(\frac{S}{\alpha D}) - 1\} . \tag{4.3}$$

Note that erfc(0) = 1 and

$$\left.\frac{dC}{dt}\right|_{t=t_d} = \frac{c_o L e^{-\frac{t_d}{\tau}}}{[(\frac{SL}{D}) - \alpha L]} \{\frac{S}{\alpha D} e^{\alpha^2 L^2 \frac{t_d}{\tau}} \operatorname{erfc}(\alpha L \sqrt{\frac{t_d}{\tau}}) - e^{(SL/D)^2 \frac{t_d}{\tau}} \operatorname{erfc}(\frac{SL}{D} \sqrt{\frac{t_d}{\tau}})\} . \tag{4.4}$$

Finally, substituting Eqs. (4.3) and (4.4) into Eq. (4.2) results in the desired PCD relationship:

$$m(S) = \frac{e^{\frac{t_d}{\tau}} (\frac{S}{\alpha D} - 1)}{\frac{S}{\alpha D} e^{\alpha^2 L^2 \frac{t_d}{\tau}} \cdot \operatorname{erfc}(\alpha L \sqrt{\frac{t_d}{\tau}}) - e^{(SL/D)^2 \frac{t_d}{\tau}} \cdot \operatorname{erfc}(\frac{SL}{D} \sqrt{\frac{t_d}{\tau}})} - 1. \tag{4.5}$$

Equation (4.5) relates the PCD signal to the surface recombination velocity, S, and the carrier lifetime, τ. Athough it is a fairly complex expression, it is essential in the determination of the surface recombination velocity. Equation (4.5) is plotted at room temperature by computer for both InP and GaAs for various values of τ. These are shown in Figures (4.2) and (4.3), respectively. For example, Figure (4.3) suggests a surface recom-

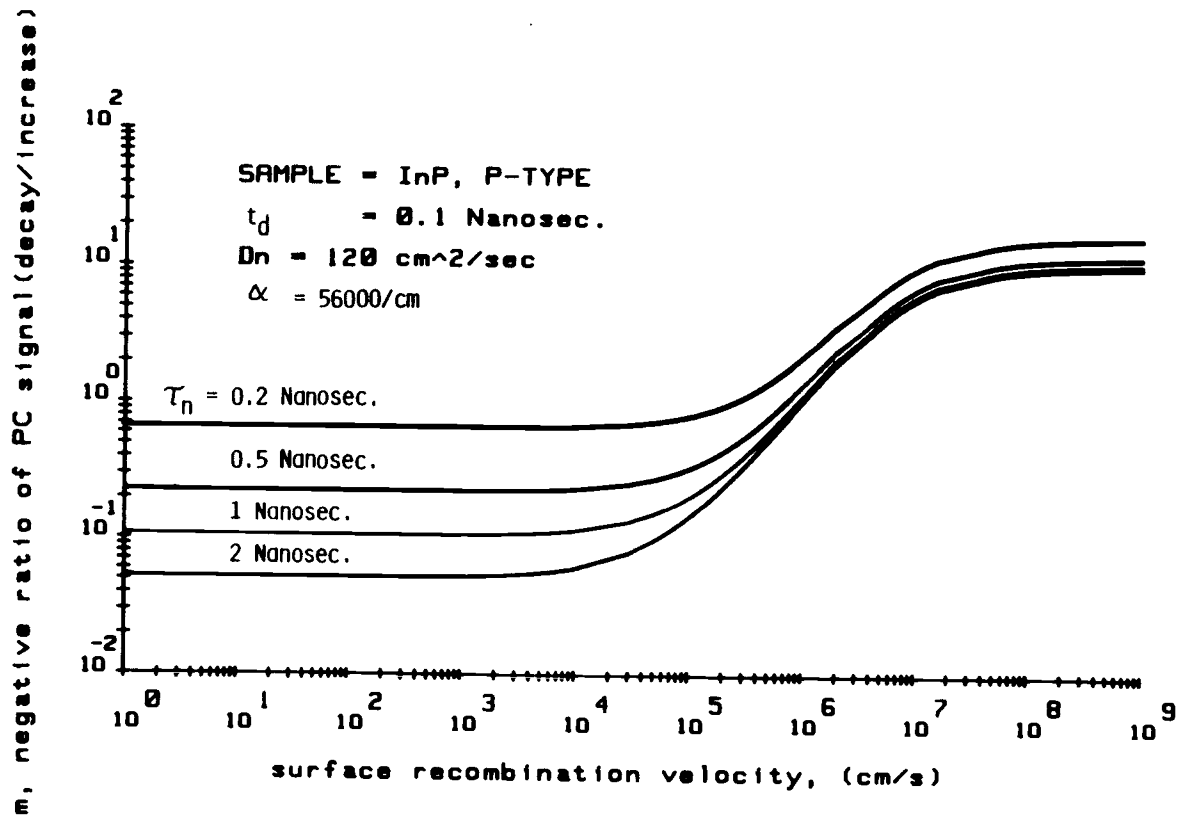

Figure 4.2. A comparison of the actual surface recombination velocity for various values of the excess minority carrier lifetime [Eq. (4.5)].

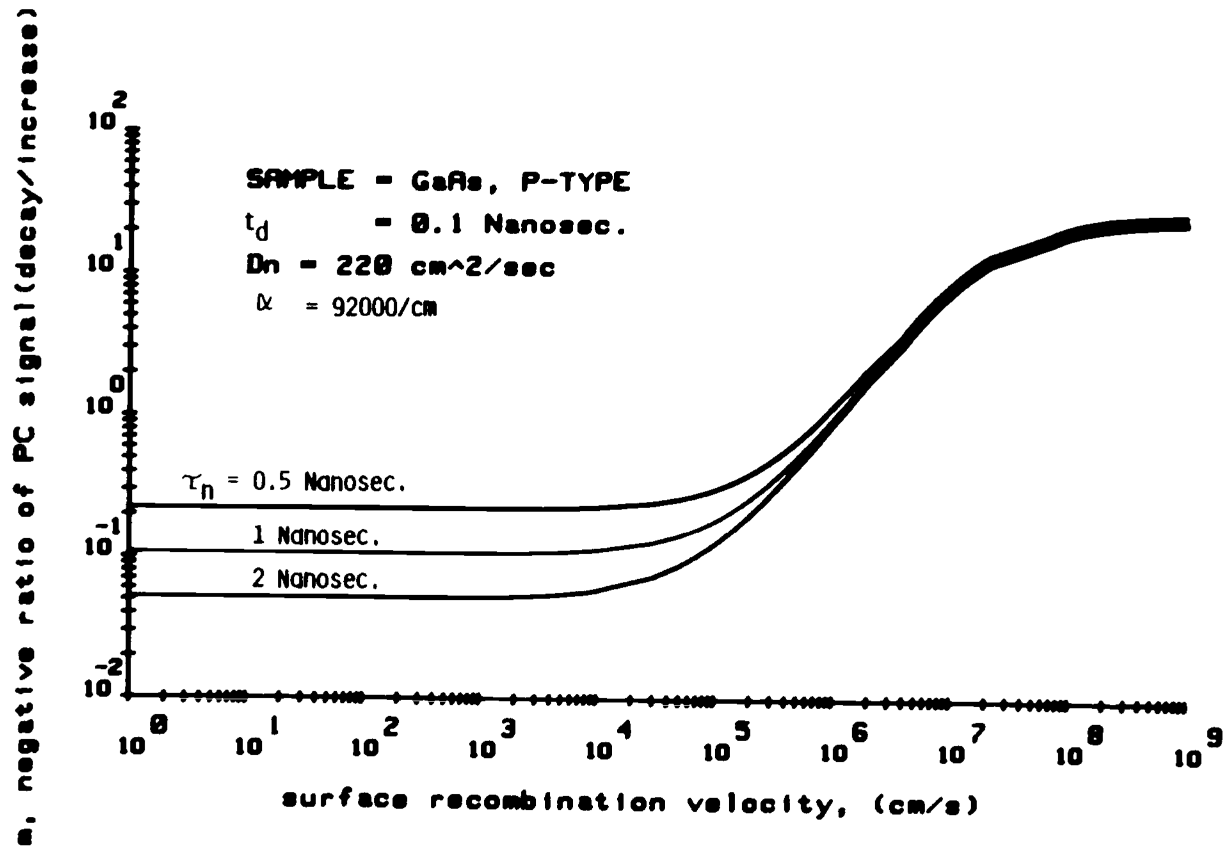

Figure 4.3. A comparison of the actual surface recombination velocity for various values of the excess minority carrier lifetime [Eq. (4.5)].

bination velocity of order 10^5 cm/s for GaAs at $\tau = 1$ nanosecond, which agrees with the result reported by H.C. Casey, et al. [15]. Note that a series expansion approximation in addition to tabulated values [16] are used in evaluation of "erfc." Figure (4.3) is reproduced [Appendix C.2, Fig. (C.1)] for an n-type GaAs sample at a similar minority carrier concentration level.

A plot of the PCD signal versus the surface recombination velocity as a function of the absorption coefficient is shown in Figures (4.4) and (4.5) for InP and GaAs, respectively. As the absorption coefficient becomes larger, the carrier pairs are induced within a thinner layer of the semiconductor surface and, thus, the surface recomination becomes more important. Similar plots are shown in Appendix [C.2] for different values of absorption coefficients.

4.2 The First Order Approximation

It is highly desirable to reduce and simplify the complications associated with the actual PCD relationship derived in Eq. (4.5). Additionally, the accuracy of this simplification must be maintained within a reasonable range. Therefore, the intention is to approximate Eq. (4.5) into a first order equation. This is accomplished using a Taylor polynomial [10] approximation method which is shown below for Si.

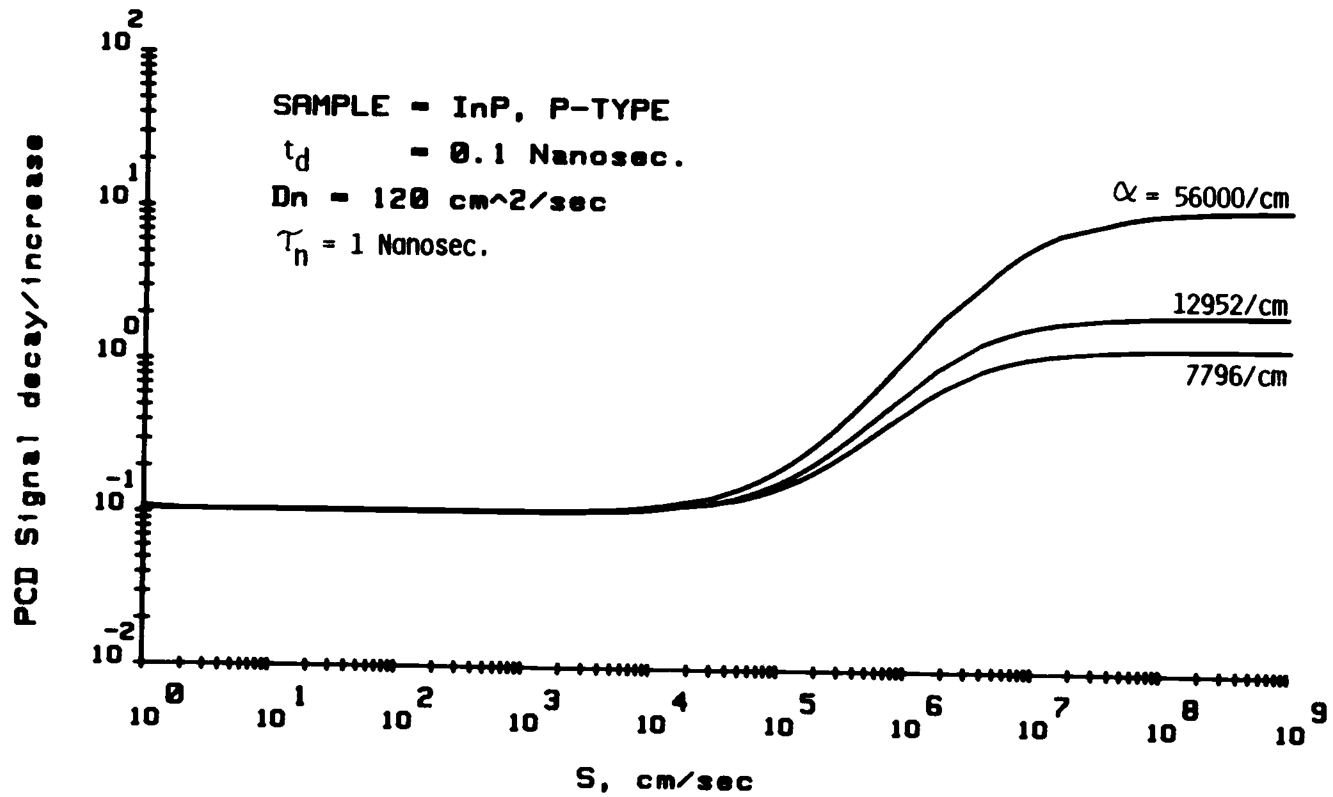

Figure 4.4. Surface recombination velocity, S, for various values of Alpha.

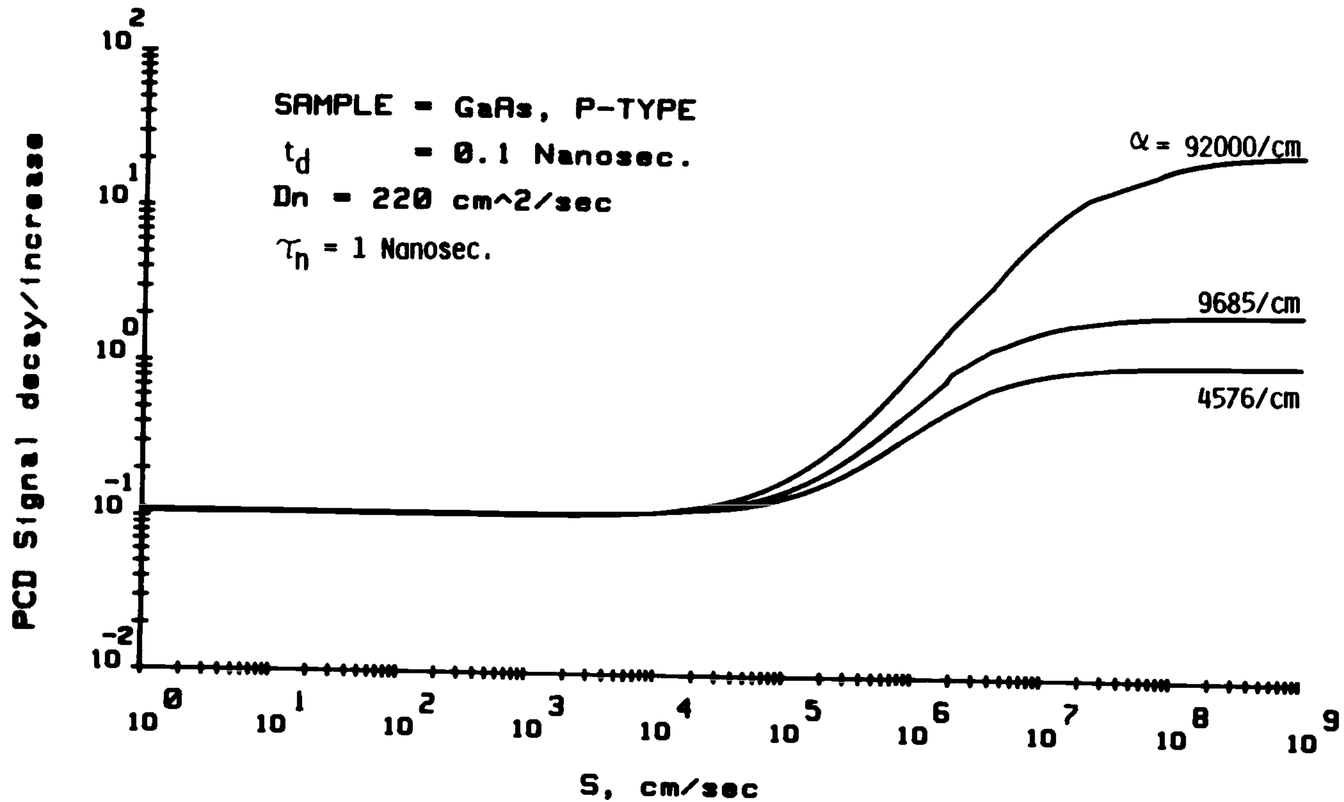

Figure 4.5. Negative ratio of the photoconductivity signal (decay/increase) versus surface recombination velocity for various values of Alpha.

4.2.1 Silicon

Eranen and Blomberg [2] have reported a first order approximation relationship between the negative ratio of the slopes of the PCD signal, m, and surface recombination velocity, S. This first order approximation [2] is given as

$$m = \alpha t_d S + \frac{t_d}{\tau} \qquad (4.6)$$

where α is the absorption coefficient of silicon at the laser wavelength, t_d is the duration of the laser pulse, and τ is the excess carrier recombination lifetime in the bulk. Equation (4.6) is plotted in Figure (4.6) for several values of τ. The importance of this relationship is that the surface recombination velocity and the minority carrier lifetime may be simultaneously extracted from a single PCD measurement.

In Section 4.1, a complete, but fairly complicated, expression was derived [Eq. (4.5)] which relates the surface recombination to the PCD signal. Figure (4.7) shows a plot of this equation for a p-type silicon.

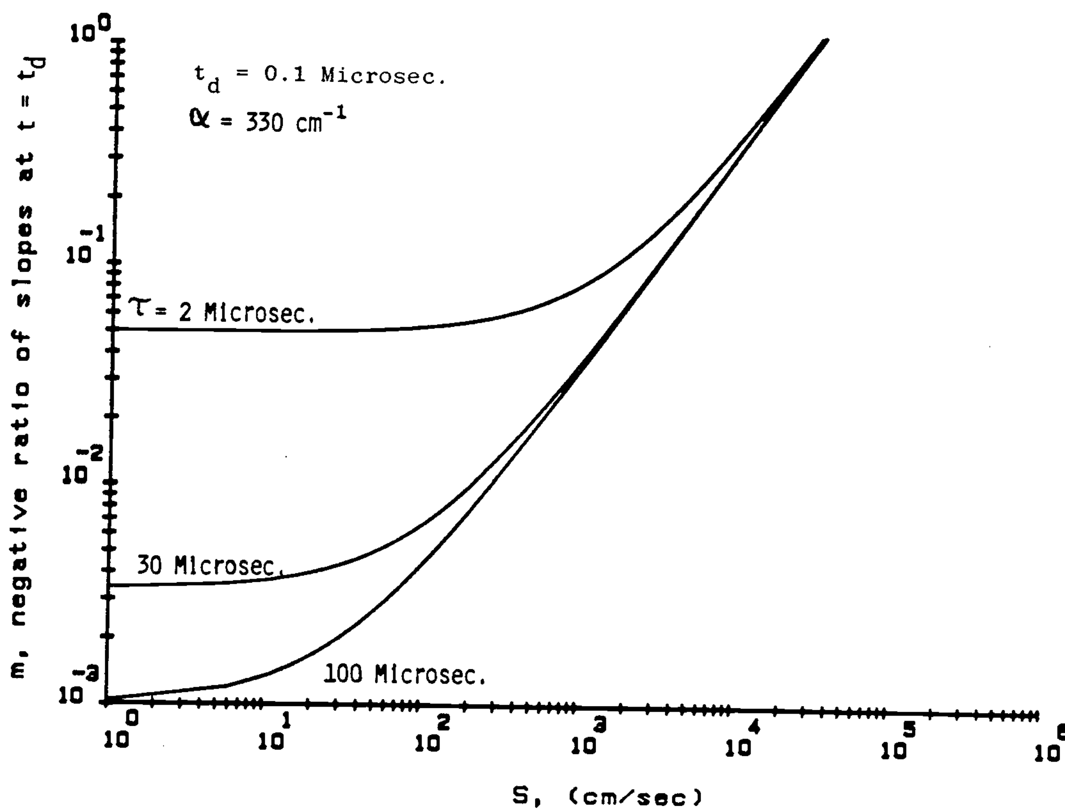

Figure 4.6. A plot of the first order approximation of m versus the surface recombination velocity.

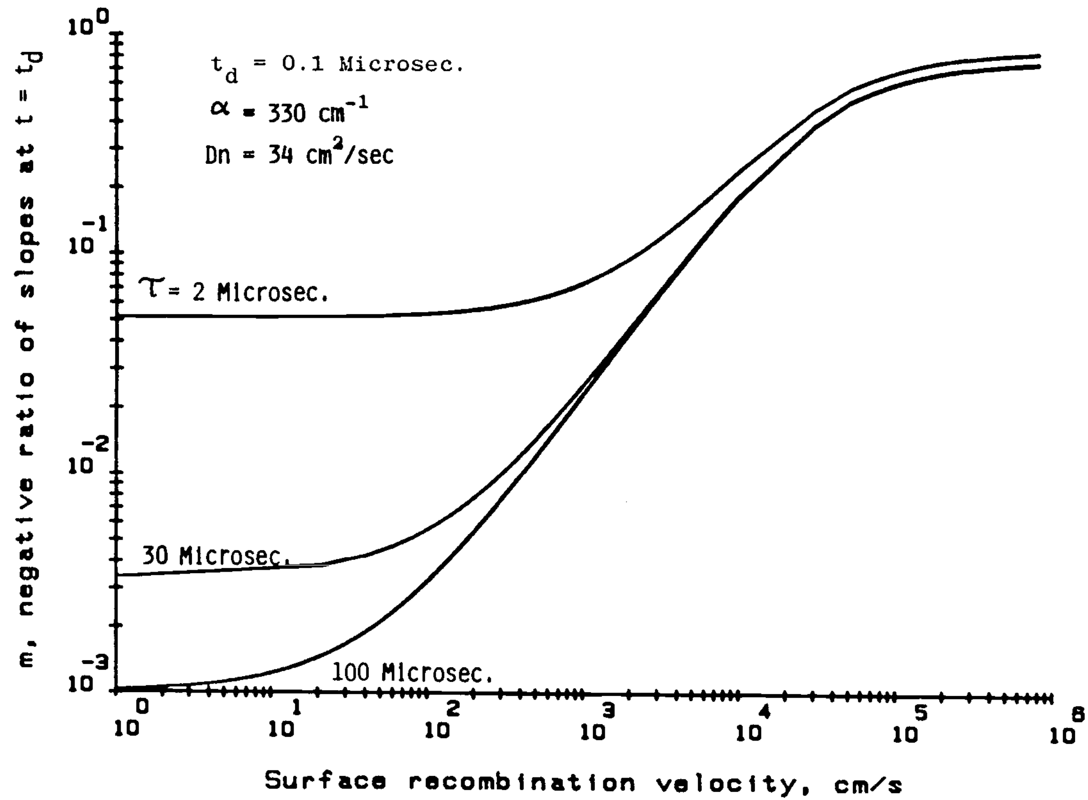

Figure 4.7. Actual variation of the negative ratio of the slopes of the PCD signal versus S for various values of bulk lifetime.

A comparison between the actual solution [Figure (4.7)] and the first order approximation [Figure (4.6)] along with a second order polynomial is shown in Figure (4.8). Clearly, there is some error associated with the first order approximation, especially when S is in the range of 10^4cm/s > S > 10^3 cm/s. This can be reduced by

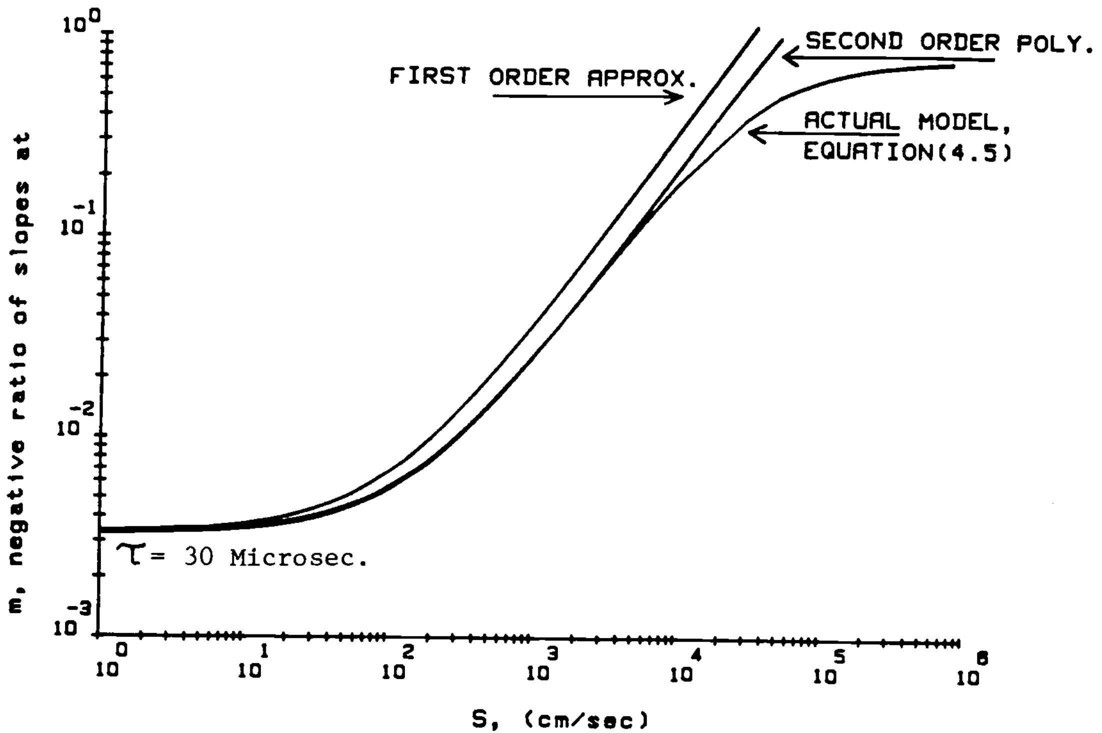

Figure 4.8. A comparison between the actual and the approximate model.

using the more complete expression derived in Eq. (4.5). The improved accuracy is obtained, however, at the price of no longer being able to use the simple first order approximation to deduce the two important physical parameters, surface recombination velocity and minority carrier lifetime.

Thus, the results of Eranen and Blomberg [2] have been reproduced for the simultaneous determination of the surface recombination velocity and minority carrier lifetime. These authors indicate that Figure (4.7) can be used directly for the determination of large values of the surface recombination velocity ($S > 5x10^4$ cm/s) and for smaller values of S, Eq. (4.6) may be applied, to obtain S and τ, simultaneously with the well-known formula [Ref. 2, Eq. (1)], given as

$$\frac{1}{\tau'} = \frac{1}{\tau} + D\left(\frac{\eta}{d}\right)^2 \qquad (4.7)$$

where τ' is the measured lifetime after the PCD signal has decayed to less than 10% of its maximum value [2] in which the excess carrier decay becomes exponential [5]. In Eq. (4.7), τ is the bulk lifetime, d is the sample thickness divided by 2, and η is given as

$$\eta \tan\eta = S\,\frac{d}{D}$$

in which S is the surface recombination velocity. This indicates the great usefulness of first order approximation.

Although Eranen and Blomberg [2] effectively point out the utility of the first order approximation, their representation is not very satisfying because they introduce this relationship as an ad hoc curve-fitting relationship. One of the accomplishments of the work presented here is the clarification of this relationship as a first order Taylor polynomial approximation to the more complete expression [Eq. (4.5)].

Using the same approach as was used for the determination of the surface recombination velocity in Si, a new equation for GaAs and InP is deduced in Section 4.2.2. The PCD relationship of Eq. (4.5) is reduced to a unique first order approximation equation that can be used to determine the surface recombination velocity and lifetime in GaAs or InP with a high degree of precision and a significant improvement in the computational simplicity.

4.2.2 **GaAs and InP**

The complete expression derived in Eq. (4.5) for the determination of surface recombination velocity in GaAs and InP is reduced to a first order analytical approximation. This approximation is accomplished using a

Taylor polynomial [10] approximation method described below.

Let

$$m(S) = a_o + a_1 S \tag{4.8}$$

where, from Eq. (4.5),

$$a_o = m(0) = e^{\frac{t_d}{\tau}} - 1 \approx \frac{t_d}{\tau}, \qquad (\frac{t_d}{\tau} << 1) \tag{4.9}$$

and

$$a_1 = \left.\frac{dm}{dS}\right|_{S = 0} \tag{4.10}$$

which can be written as

$$a_1 = -\frac{1}{\alpha D} e^{\frac{t_d}{\tau}} + e^{\frac{t_d}{\tau}} [\frac{1}{\alpha D} e^{\alpha^2 L^2 \frac{t_d}{\tau}} \operatorname{erfc}(\alpha L \sqrt{\frac{t_d}{\tau}})$$

$$+ \frac{2L}{D} \sqrt{\frac{t_d}{\tau\pi}}]. \tag{4.11}$$

Since the absorption coefficient, α, is very large for InP or GaAs, Eq. (4.11) can be reduced to

$$a_1 = -\frac{1}{\alpha D} e^{\frac{t_d}{\tau}} + e^{\frac{t_d}{\tau}} (\frac{2L}{D} \sqrt{\frac{t_d}{\tau\pi}}) . \tag{4.12}$$

Note that $\operatorname{erfc}(\infty) = 0$.

Equation (4.12) can be approximated [Appendix C.3] to

$$a_1 \simeq 2\sqrt{\frac{t_d}{D\pi}}\ , \qquad \left(\frac{t_d}{\tau} \ll 1\right) \tag{4.13}$$

Finally, substituting Eqs. (4.9) and (4.13) into Eq. (4.8) gives the desired first order model:

$$m(S) \approx 2\sqrt{\frac{t_d}{D\pi}} \cdot S + \frac{t_d}{\tau}\ . \tag{4.14}$$

It is important to recognize that the first order approximation is different for GaAs and InP [Eq. (4.14)] than it is for silicon [Eq. (4.6)]. This difference is mainly due to the fact that the absorption coefficient, α, is much larger and the minority carrier lifetime is much smaller in GaAs and InP than in silicon. This first order approximation derived in Eq. (4.14) is a very important relationship because it enables a simultaneous determination of surface recombination velocity and the minority carrier lifetime from the experimental value of the PCD measurement, m. A comparison of the first order approximation to the complete expression is shown in Figure (4.9) for various values of τ for a p-type GaAs at room temperature. This comparison is also shown [Appendix C.2, Fig. (C.4)] for n-type GaAs. Subsequently, Figure (4.9) is reproduced [Appendix C.2, Fig. (C.5)] for a different doping concentration and, consequently, a different value of

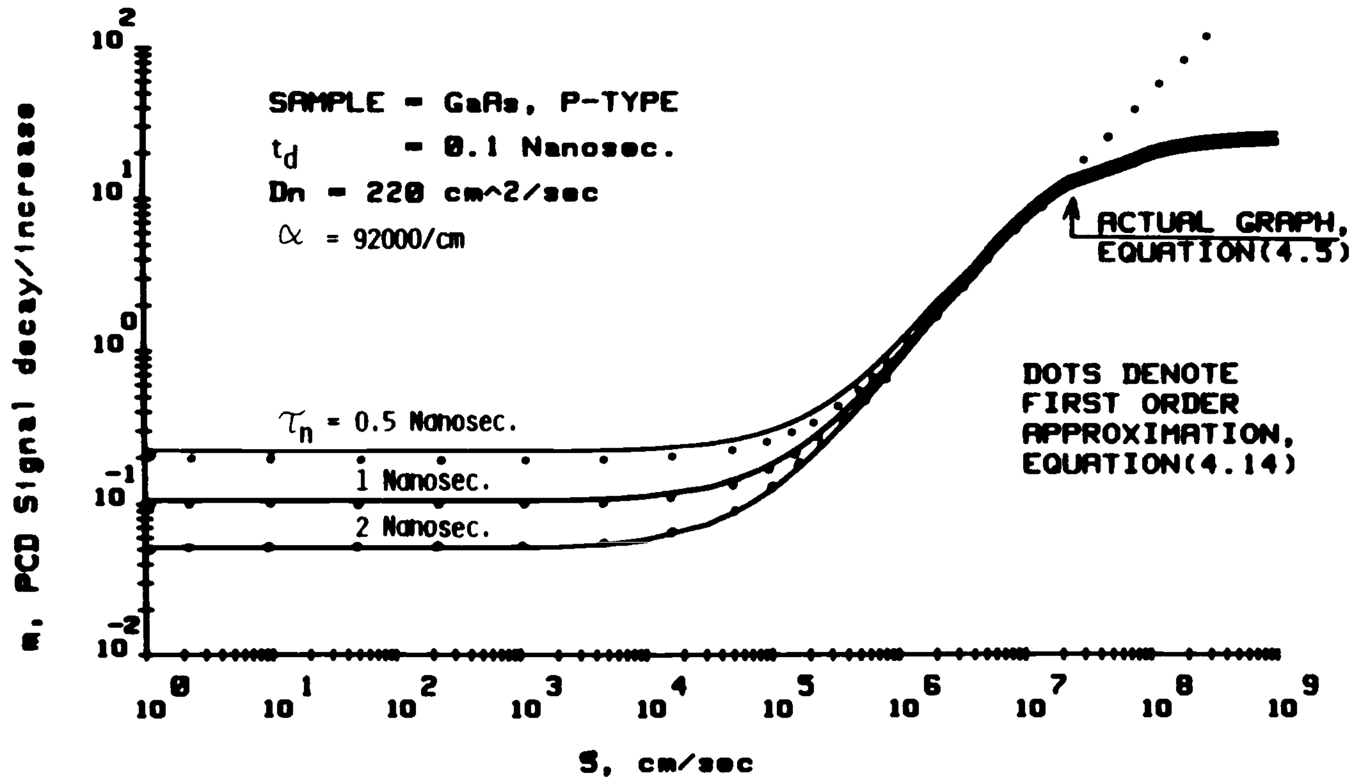

Figure 4.9. A plot of the first order approximation model against the actual variation of the surface recombination velocity, S.

mobility. A similar plot is shown for InP in Figure (4.10).

These figures provide a relatively accurate method for the determination of the surface recombination velocity with a great reduction in the complexity of analysis. For example, the actual graph in Figure (4.10) can be used directly for the evalaution of large values ($S > 10^7$ cm/s) of the surface recombination velocity in InP. This is because in this range, surface recombination velocity is nearly independent of the lifetime. However, for smaller values of S (10^4 cm/s $< S < 10^7$ cm/s), Eq. (4.14) is used simultaneously with Eq. (4.7) to provide the appropriate values for S and τ. As observed from Figures (4.9) and (4.10), the first order approximation equation yields a good fit for $S < 5 \times 10^6$ cm/s. Evaluating the surface recombination velocity from this analytical approximation may result in an underestimation of about 10%. This can be overcome by using the more complex expression derived in Eq. (4.5).

In summary, the surface recombination velocity, S, and the bulk minority carrier lifetime, τ, of GaAs or InP may be simultaneously determined from an experimental measurement of the PCD signal. For large values of S, the surface recombination velocity is nearly independent of the lifetime and may be evaluated directly from the PCD signal versus surface recombination velocity plot. The

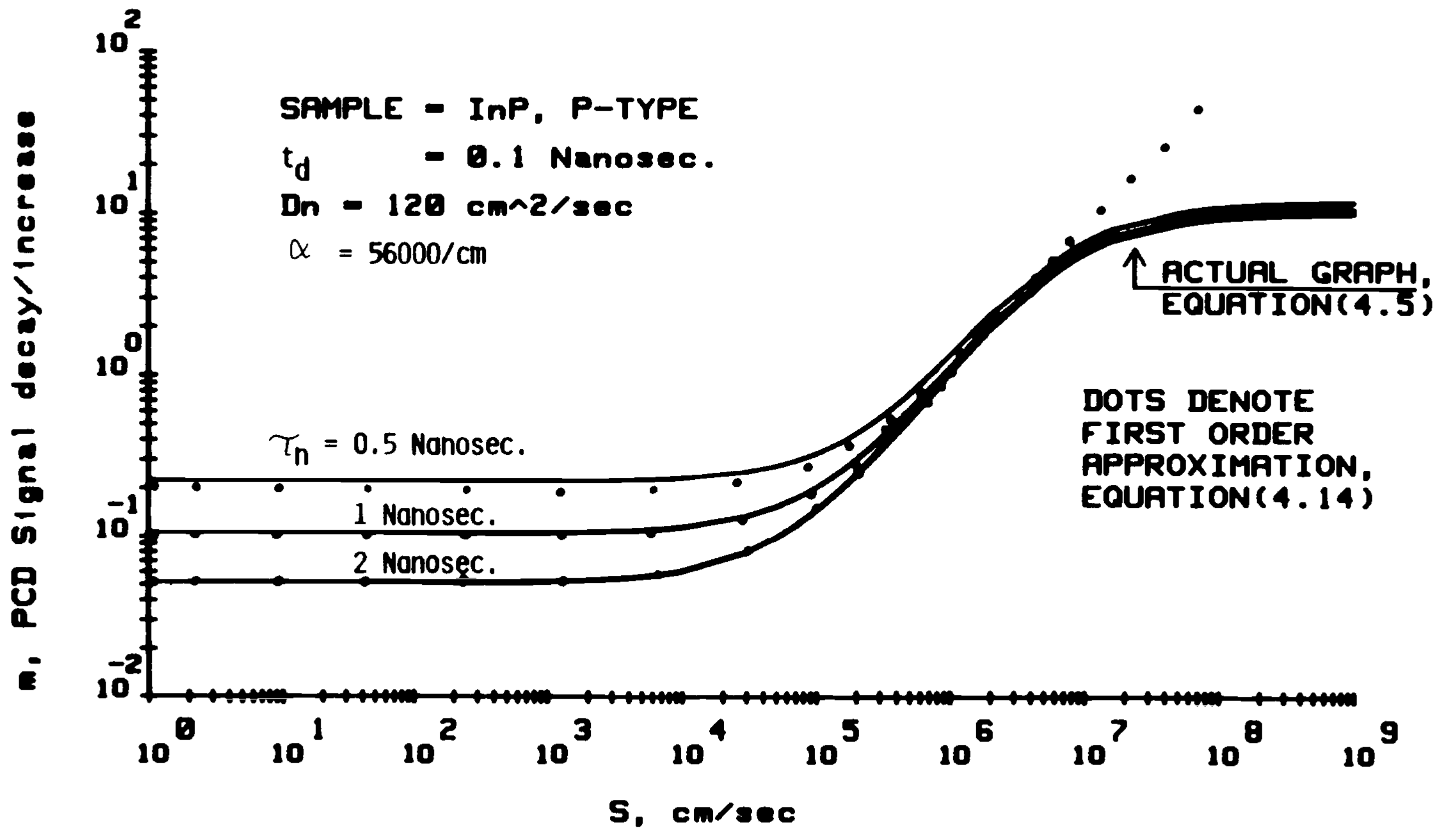

Figure 4.10. A plot of the first order approximation model against the actual variation of the surface recombination velocity, S.

bulk minority carrier lifetime may also be found by measuring the long time scale decay constant along with Eq. (4.7). For smaller values of the surface recombination velocity, Eq. (4.7) is again employed in conjunction with the first order approximation [Eq. (4.14)] to obtain S and τ. The first order approximation for materials with small optical absorption coefficients and long lifetimes (e.g., silicon) is given by Eq. (4.6) while Eq. (4.14) is used for materials with a very large optical absorption coefficient and small minority carrier lifetime (e.g, p-type GaAs or InP).

CHAPTER 5

CONCLUSIONS AND FUTURE WORK

An analytical model was developed to analyze the data obtained from a nondestructive photoconductivity decay (PCD) technique for the determination of the surface recombination velocity, S, and minority carrier lifetime, τ, in GaAs and InP. Some of the major accomplishments in this thesis are:

1. A complex expression was derived to relate S and τ to the experimental parameter, m, obtained from a PCD measurement.
2. The complex expression was reduced to a first order approximation equation which greatly simplifies the analysis and provides a methodology for the determination of S and τ.
3. The first order approximation found for GaAs and InP is different, however, than that for Si. This is because of the much larger absorption coefficient, α, and much smaller lifetime, τ, of the III-V compound semiconductors compared to Si.
4. A computer simulation was performed to compare the first order approximation to the more complex model. The first order

approximation was shown to be quite accurate for most purposes.

5. The form of the first order approximation for GaAs and InP is independent of the semiconductor mobility. Thus, the simulation is equally valid for p- and n-type semiconductors and its validity is independent of the doping density. This is associated with the larger α and smaller τ of the III-V compound semiconductors, used to obtain the first order approximation model.
6. Large values of surface recombination velocity are nearly independent of the lifetime, because for larger α the generation takes place nearer to the surface.
7. If the PCD measurement were performed successfully, many applications arise for noncontact evaluation of S and τ. For example, process development for dielectric deposition on compound semiconductors, high-efficiency Si solar cells [17], photodetectors [18], and so forth [15,19] could be optimized in a much more efficient manner.

Although an approach for the determination of S and τ in GaAs and InP has been presented in this thesis, there are several important issues to consider for further development:

1. The analysis provided here was based on the assumption of low level injection (i.e, the excess carrier concentration is much less than the equilibrium majority carrier concentration). In high injection (i.e., the excess carrier concentration is comparable with majority carrier concentration), the carrier lifetime will be a function of the excess carrier density and, consequently, the simple term for recombination used in continuity equation will not be the same. Additionally, diffusion and drift are coupled in the case of high injection and the ambipolar diffusivity and mobility must be used. The issue of high injection is particularly significant to the case of semi-insulating GaAs and InP because of their very small carrier densities, 10^6-$10^7/cm^3$.
2. An obvious extension of the work reported in this thesis is to perform the PCD measurement with GaAs and InP. In order to

maintain low level injection, high doping densities and low laser powers should be employed. Additionally, the laser pulse ($h\nu > E_g$) duration must be much less than the minority carrier lifetime. This suggests a pulse duration of less than about 100 picoseconds. The PCD signal must also be detected on this time scale.

3. The analysis presented in this thesis should also be extended to the ternary III-V compound semiconductor, $In_{0.53}Ga_{0.47}As$, an extremely important material for light-wave communications.

BIBLIOGRAPHY

[1] Carl W. Wilmsen, Physics and Chemistry of III-V Compound Semiconductor Interfaces, pp. 339-342.

[2] S. Eranen and M. Blomberg, "Simultaneous Measurement of Recombination Lifetime and Surface Recombination Velocity," Journal of Applied Physics, 56(8), 15 October 1984, pp. 2372-2374.

[3] M.S. Tyagi, J.F. Nus, and R.J. Van Overstraeten, "Effect of Surface Recombination on the Transient Decay of Excess Carriers Produced by Short Wavelength Laser Pulses," Solid-State Electronics, Vol. 25, No. 5, 1982, pp. 411-415.

[4] A.S. Grove, Physics and Technology of Semiconductor Devices, John Wiley & Sons, Inc., 1967, pp. 121-127, 137-140.

[5] J.P. McKelvey, Solid State and Semiconductor Physics, Krieger, Florida, 1982, pp. 346-361.

[6] E. Kreyszig, Advanced Engineering Mathematics, John Wiley & Sons, 1979, pp. 63-113.

[7] S.M. Selby, Standard Mathematical Tables, The Chemical Rubber Co., CRC, 1969, pp. 499-518, 395-398.

[8] P.Z. Peebles, Jr., Probability, Random Variables, and Random Signal Principles, McGraw-Hill Book Co., 1980, pp. 42-45.

[9] F. Oberhettinger and L. Badii, Table of Laplace Transforms, Springer-Verlag, 1973, p. 259.

[10] R.L. Burden, J.D. Fairses, and A.C. Reynolds, Numerical Analysis, Prindle, Weber & Schmidt, 1978, pp. 74-80.

[11] S.J. Fonash, Solar Cell Devices Physics, Academic Press, 1981, p. 26.

[12] S.M. Sze, Physics of Semiconductor Devices, John Wiley & Sons, 1981, p. 42.

[13] J.I. Pankove, Optical Processes in Semiconductors, Dover Publications, Inc., 1971, pp. 85-91.

[14] R.K. Willardson and A.C. Beer, Semiconductors and Semimetals, Academic Press, 1967, Vol. 3, pp. 499-543.

[15] H.C. Casey, Jr., A.Y. Cho, and P.W. Foy, "Reduction of Surface Recombination Current in GaAs p-n Junctions," Applied Physics Letters, 34(9), 1 May 1979, pp. 594-596.

[16] U.S. Department of Commerce, Tables of the Error Function and Its Derivative, National Bureau of Standards, Applied Mathematics Series, No. 41, October 1954, pp. 1-302.

[17] B.H. Rose and H.T. Weaver, "Determination of Effective Surface Recombination Velocity and Minority Carrier Lifetime in High-Efficiency Si Solar Cells," Journal of Applied Physics, 54(1), January 1983, pp. 238-247.

[18] Thomas P. Pearsall, "$Ga_{0.47}In_{0.53}As$: A Ternary Semiconductor for Photodetectors Applications," IEEE Journal of Quantum Electronics, Vol. QE-16, No. 7, July 1980, pp. 709-712.

[19] C.H. Henry, R.A. Logan, and F.R. Merritt, "The Effect of Surface Recombination on Current in $Al_xGa_{1-x}As$ Heterojunctions," Journal of Applied Physics, 49(6), June 1978, pp. 3530-3542.

APPENDICES

APPENDIX A

THE CONTINUITY EQUATION

A complete mathematical solution to the time-dependent minority carrier continuity equation similar to the analysis reported by Tyagi et al. [3] is presented in this appendix. From Eq. (3.2),

$$\frac{d^2(\Delta n)}{dx^2} - \frac{\Delta n}{D\tau} + \frac{C_g(x)}{D} = \frac{1}{D}\frac{d(\Delta n)}{dt} \qquad (A.1)$$

where

$$C_g(x) = \begin{cases} c_o e^{-\alpha x} & \text{for } t < t_d \\ 0 & \text{for } t > t_d \end{cases} \qquad (A.2)$$

with boundary conditions

$$1) \quad D \left.\frac{\partial(\Delta n)}{\partial x}\right|_{x=0} = S \cdot \Delta n(0,t)$$

$$2) \quad \Delta n(x,t)\big|_{t=0} = 0 \qquad (A.3)$$

$$3) \quad \Delta n(x,t)\big|_{x=\infty} = 0$$

$C_g(x)$ can be written as

$$C_g(x) = c_o e^{-\alpha x}[1 - U(t - t_d)] \tag{A.4}$$

Note that

$$U(t) = \begin{cases} 1 \text{ if } t > 0 \\ 0 \text{ if } t < 0 \end{cases}$$

is a unit step; therefore,

$$U(t - t_d) = \begin{cases} 1 \text{ if } t > t_d \\ 0 \text{ if } t < t_d \ . \end{cases} \tag{A.5}$$

Equation (A.1) can be solved using Laplace transformation in the **s** domain [7]. Note that

$$\mathbf{L}[\frac{df}{dt}] = \mathbf{s}\ \mathbf{L}(f) - f(0) \ .$$

Then, the Laplace transform of Eq. (A.1) with respect to t, using the initial condition in Eq. (A.3),

$$\frac{\partial^2 N}{\partial x^2} - \frac{N}{D\tau} + \frac{c_o e^{-\alpha x}}{D} (\frac{1}{\mathbf{s}} - \frac{e^{-\mathbf{s}t_d}}{\mathbf{s}}) = \frac{\mathbf{s}N}{D} \ . \tag{A.6}$$

After rearranging,

$$\frac{\partial^2 N}{\partial x^2} - (\frac{\mathbf{s}\tau + 1}{D\tau})\ N = \frac{-c_o}{D\mathbf{s}} (1 - e^{-\mathbf{s}t_d})\ e^{-\alpha x} \tag{A.7}$$

Let

$$\gamma = \sqrt{\left(\frac{s\tau+1}{D\tau}\right)} \text{ and } \beta = \frac{-c_o}{Ds}\left(1 - e^{-st_d}\right) . \quad (A.8)$$

Substituting into Eq. (A.7) then,

$$\frac{\partial^2 N}{\partial x^2} - \gamma^2 N - \beta e^{-\alpha x} = 0 . \quad (A.9)$$

The homogeneous solution [6] is

$$\frac{\partial^2 N}{\partial x^2} - \gamma^2 N = 0$$

or

$$N_h(x) = K_1 e^{\gamma x} + K_2 e^{-\gamma x} \quad (A.10)$$

and the particular solution [6] is

$$N_p(x) = K_3 e^{-\alpha x} . \quad (A.11)$$

Taking the second derivative of $N_p(x)$ and substituting it in Eq. (A.9), it can be shown that

$$K_3 = \frac{\beta}{\alpha^2 - \gamma^2} e^{-\alpha x} .$$

Finally, the total solution [6] is

$$N(x,s) = K_1 e^{\gamma x} + K_2 e^{-\gamma x} + \frac{\beta}{\alpha^2 - \gamma^2} e^{-\alpha x} . \quad (A.12)$$

Using the boundary conditions

$$N(\infty,t) = 0 \rightarrow K_1 = 0$$

and

$$\left.\frac{\partial N}{\partial x}\right|_{x=0} = \frac{S}{D} N(0,s) \quad (A.13)$$

It is found that

$$\left.\left(-K_2 \gamma e^{-\gamma x} - \frac{\alpha\beta}{\alpha^2 - \gamma^2} e^{-\alpha x}\right)\right|_{x=0} = \frac{S}{D} \left(K_2 + \frac{\beta}{\alpha^2 - \gamma^2}\right) . \quad (A.14)$$

Simplifying and rearranging results in

$$K_2 = \beta \frac{\frac{-\alpha}{\alpha^2 - \gamma^2} - \frac{S}{D} \frac{1}{\alpha^2 - \gamma^2}}{\frac{S}{D} + \gamma} . \quad (A.15)$$

Substituting for K_1 and K_2 in Eq. (A.12) and factoring out β, gives

$$N(x,s) = \beta\left[\frac{\frac{-\alpha}{\alpha^2 - \gamma^2} - \frac{S}{D} \frac{1}{\alpha^2 - \gamma^2}}{\frac{S}{D} + \gamma} \cdot e^{-\gamma x} + \frac{1}{\alpha^2 - \gamma^2} e^{-\alpha x}\right] .$$

(A.16)

Substituting Eq. (A.8) into (A.16) for β,

$$N(x,s) = \left[\frac{-c_o}{Ds} \cdot \frac{\frac{-\alpha}{\alpha^2-\gamma^2} - \frac{S}{D}\frac{1}{\alpha^2-\gamma^2}}{\frac{S}{D}+\gamma} \cdot e^{-\gamma x} - \frac{\frac{c_o}{Ds}}{\alpha^2-\gamma^2} e^{-\alpha x}\right](1 - e^{-st_d}) \ . \qquad (A.17)$$

The next step is to find the excess carrier concentration, $N(x,t)$ which is the inverse Laplace transform of Eq. (A.17). For simplicity Eq. (A.17) may be broken into two parts, $C_1(x,s)$ and $C_2(x,s)$. These are represented as just C_1 and C_2.

Let

$$C_1 = \frac{-c_o}{Ds} \cdot \frac{\frac{-\alpha}{\alpha^2-\gamma^2} - \frac{S}{D}\frac{1}{\alpha^2-\gamma^2}}{\frac{S}{D}+\gamma} \cdot e^{-\gamma x} \qquad (A.18)$$

which may be simplified to

$$C_1 = \frac{-c_o\left(\alpha + \frac{S}{D}\right) e^{-\gamma x}}{D^2(\gamma^2-\alpha^2)\left(\gamma + \frac{S}{D}\right)\left(\gamma^2 - \frac{1}{L^2}\right)} \qquad (A.19)$$

where $L = \sqrt{D\tau}$ is the diffusion length.

Let

$$C_2 = \frac{-c_o}{Ds(\alpha^2 - \gamma^2)} e^{-\alpha x} \quad . \qquad (A.20)$$

Substituting Eq. (A.8) for γ results in

$$C_2 = \frac{c_o \tau}{s[s\tau + (1 - L^2 \alpha^2)]} e^{-\alpha x} \quad .$$

Therefore, Eq. (A.17) may be written as

$$N(x,s) = (C_1 + C_2)(1 - e^{-st_d}) \quad . \qquad (A.22)$$

Let N(x,t) represent the inverse Laplace transform of N(x,s). Then it is necessary to find the inverse Laplace of C_1 and C_2 and add the results. Therefore,

$$C_1 = - \frac{c_o(\alpha + \frac{S}{D}) \, e^{-\gamma x}}{D^2(\gamma^2 - \frac{1}{L^2})(\gamma^2 - \alpha^2)(\gamma + \frac{S}{D})} \quad .$$

Using partial fractions,

$$C_1 = \frac{-c_o(\alpha + \frac{S}{D})}{D^2} e^{-\gamma x} \left[\frac{A}{\gamma - \frac{1}{L}} + \frac{B}{\gamma + \frac{1}{L}} + \frac{E}{\gamma - \alpha} + \frac{F}{\gamma + \alpha} + \frac{G}{\gamma + \frac{S}{D}} \right] \quad .$$

$$(A.23)$$

It can be shown that

$$A = \frac{L^4}{-2(\alpha^2L^2 - 1)(\frac{SL}{D} + 1)} \quad , \quad B = \frac{L^4}{2(\alpha^2L^2 - 1)(\frac{SL}{D} - 1)}$$

$$E = \frac{L^3}{2\alpha(\alpha^2L^2 - 1)(\frac{SL}{D} + \alpha L)} \quad , \quad F = \frac{L^3}{-2\alpha(\alpha^2L^2 - 1)(\frac{SL}{D} - \alpha L)}$$

and

$$G = \frac{-L^4}{((\frac{SL}{D})^2 - 1)(\alpha^2L^2 - (\frac{SL}{D})^2)} \ . \tag{A.24}$$

Now the inverse Laplace transform of the first term in Eq. (A.23) is

$$\mathbf{L}^{-1}[\frac{e^{-\gamma x}}{\gamma - \frac{1}{L}}] = \mathbf{L}^{-1}[\frac{\sqrt{D}\ e^{-x\sqrt{\frac{1}{D}}\ \cdot\ \sqrt{s + \frac{1}{\tau}}}}{\sqrt{s + \frac{1}{\tau}} - \frac{\sqrt{D}}{L}}] \tag{A.25}$$

Employing the following property [9]

$$\mathbf{L}^{-1}\ \frac{e^{-a\sqrt{s}}}{\sqrt{s} + b} = (\sqrt{\pi t})^{-1}\ e^{-\frac{a^2}{4t}} - b.e^{(ab + b^2t)}$$

$$\cdot\ \mathrm{erfc}(\frac{1}{2}\ a\sqrt{t}^{\ -1} + b\sqrt{t}) \tag{A.26}$$

and from the shifting theorem:

$$e^{-\alpha s}F(s) \rightarrow L\{f(t-\alpha)\,U(t)\}$$

$$(A.27)$$

$$F(s-\alpha) \rightarrow L\{e^{\alpha t}\,f(t)\}\ .$$

By using Eq. (A.27), Eq. (A.25) simplifies to:

$$\sqrt{D}\cdot e^{-\frac{t}{\tau}}\,L^{-1}\,\frac{e^{-x\sqrt{\frac{1}{D}}\cdot\sqrt{s}}}{\sqrt{s}+\frac{\sqrt{D}}{L}}$$

which by using the formula in (A.26) and letting $L = \sqrt{D\tau}$ it can be shown that

$$\sqrt{D}\cdot e^{-\frac{t}{\tau}}\,L^{-1}\,\frac{e^{-x\sqrt{\frac{1}{D}}\cdot\sqrt{s}}}{\sqrt{s}+\frac{\sqrt{D}}{L}} = \sqrt{D}\cdot e^{-\frac{t}{\tau}}\,\{\frac{1}{\sqrt{\pi t}}\,e^{-\frac{x^2}{4Dt}}$$

$$+\frac{\sqrt{D}}{L}\,[e^{-\frac{x}{L}}\cdot e^{\frac{t}{\tau}}\cdot \mathrm{erfc}(\frac{x}{2\sqrt{Dt}}-\sqrt{\frac{t}{\tau}})]\}\ . \qquad (A.28)$$

So, for the A and B terms in Eq. (A.23), after taking the inverse Laplace transform and simplifying gives,

$$\frac{c_o(\alpha + \frac{S}{D})L^3}{2D} e^{-\frac{t}{\tau}} \left[\frac{1}{(\alpha^2L^2 - 1)} \left(\frac{e^{-\frac{x}{L}}}{\frac{SL}{D} + 1} \operatorname{erfc}\left(\frac{x}{2\sqrt{Dt}} - \sqrt{\frac{t}{\tau}}\right)\right.\right.$$

$$\left.\left. + \frac{e^{\frac{x}{L}}}{(\frac{SL}{D} - 1)} \cdot \operatorname{erfc}\left(\frac{x}{2\sqrt{Dt}} + \sqrt{\frac{t}{\tau}}\right)\right) e^{\frac{t}{\tau}} \right] . \tag{A.29}$$

A similar procedure can be used to find the inverse Laplace transform for the E, F, and G terms in Eq. (A.23). Therefore, the final result is

$$L^{-1}[C_1] = \frac{c_o(\alpha + \frac{S}{D})L^3}{2D} e^{-\frac{t}{\tau}} \left[\frac{1}{(\alpha^2L^2 - 1)} \left(\frac{e^{-\frac{x}{L}}}{(\frac{SL}{D} + 1)}\right.\right.$$

$$\left.\left. \cdot \operatorname{erfc}\left(\frac{x}{2\sqrt{Dt}} - \sqrt{\frac{t}{\tau}}\right) + \frac{e^{\frac{x}{L}}}{(\frac{SL}{D} - 1)} \operatorname{erfc}\left(\frac{x}{2\sqrt{Dt}} + \sqrt{\frac{t}{\tau}}\right)\right) e^{\frac{t}{\tau}} \right]$$

$$- \frac{c_o(\alpha + \frac{S}{D})L^3}{2D} e^{-\frac{t}{\tau}} \left[\frac{e^{\alpha^2L^2 \frac{t}{\tau}}}{\alpha^2L^2 - 1} \left(\frac{e^{-\alpha x}}{(\frac{SL}{D} + \alpha L)} \operatorname{erfc}\left(\frac{x}{2\sqrt{Dt}}\right.\right.\right.$$

$$\left.\left.\left. - \alpha L \sqrt{\frac{t}{\tau}}\right) + \frac{e^{\alpha x}}{\frac{SL}{D} - \alpha L} \operatorname{erfc}\left(\frac{x}{2\sqrt{Dt}} + \alpha L \sqrt{\frac{t}{\tau}}\right)\right)\right]$$

$$+ \frac{c_o(\alpha + \frac{S}{D})L^3}{2D} e^{-\frac{t}{\tau}} \left[-2\left(\frac{SL}{D}\right) \frac{e^{(\frac{S}{D})x}}{((\frac{SL}{D})^2 - 1)(\alpha^2L^2 - (\frac{SL}{D})^2)}\right.$$

$$\left. \cdot \operatorname{erfc}\left(\frac{x}{2\sqrt{Dt}} + \frac{SL}{D} \sqrt{\frac{t}{\tau}}\right) e^{(\frac{SL}{D})^2 \frac{t}{\tau}}\right] \tag{A.30}$$

The inverse Laplace transform of C_2 can be found as

$$\mathbf{L}^{-1}[C_2] = \mathbf{L}^{-1}\{\frac{c_o \tau\ e^{-\alpha x}}{s[s\tau + (1 - \alpha^2 L^2)]}\}$$

$$= c_o \tau\ e^{-\alpha x}\ L^{-1}[\frac{1}{s} \cdot \frac{1}{s\tau + (1 - \alpha^2 L^2)}] \ . \qquad (A.31)$$

Using partial fractions,

$$\frac{1}{s} \cdot \frac{1}{s\tau + (1 - \alpha^2 L^2)} = \frac{A}{s} + \frac{B}{s\tau + (1 - \alpha^2 L^2)}$$

where

$$A = \frac{1}{1 - \alpha^2 L^2}$$

and

$$B = - \frac{\tau}{1 - \alpha^2 L^2} \ .$$

Substituting into (A.31), the final result is

$$L^{-1}\ [C_2] = \frac{c_o \tau e^{-\alpha x}}{1 - \alpha^2 L^2}\ [1 - e^{-(1 - \alpha^2 L^2)\ \frac{t}{\tau}}] \ . \qquad (A.32)$$

Having found the inverse Laplace transform of C_1 and C_2, N(x,t) can be found by letting

$$C(x,t) = \mathbf{L}^{-1}[C_1(x,\mathbf{s})] + \mathbf{L}^{-1}[C_2(x,\mathbf{s})] \tag{A.33}$$

and then from Eq. (A.22)

$$N(x,\mathbf{s}) = C(x,\mathbf{s}) - e^{-\mathbf{s}t_d} C(x,\mathbf{s}) \tag{A.34}$$

and by using the shifting theorem, the excess carrier concentration N(x,t) can be written as

$$N(x,t) = C(x,t)\,U(t) - C[x,\,(t - t_d)]\,U(t - t_d) \tag{A.35}$$

or

$$N(x,t) = \begin{cases} C(x,t) & \text{if } t < t_d \\ C(x,t) - C[x,(t - t_d)] & \text{if } t > t_d \end{cases} \tag{A.36}$$

where C(x,t) is shown in Eq. (A.33) and is similar to Eq. (14) of reference [3].

APPENDIX B

DERIVATION OF THE TIME-DEPENDENT PCD SIGNAL

In order to derive Eq. (3.9), which is equivalent to the solution of Ref. 2 [Eq. 2b)], it is necessary to substitute Eqs. (A.32) and (A.30) into (A.33) and integrate over the thin layer of the effective diffusion length, ℓ, at the surface. Equation (A.33) is very complex. To simplify the integration, this equation is broken up into four parts, F_1, F_2, F_3, and F_4 which can be written as

$$F_1 = \frac{c_o L^3}{2D} (\alpha + \frac{S}{D}) e^{-\frac{t}{\tau}} [\frac{1}{(\alpha^2 L^2 - 1)} \cdot \frac{e^{\frac{t}{\tau}}}{(\frac{SL}{D} + 1)} \cdot e^{-\frac{x}{L}}$$

$$\cdot \operatorname{erfc}(\frac{x}{2\sqrt{Dt}} - \sqrt{\frac{t}{\tau}}) + \frac{1}{(\alpha^2 L^2 - 1)} \cdot \frac{1}{(\frac{SL}{D} - 1)}$$

$$\cdot e^{\frac{t}{\tau}} \cdot e^{\frac{x}{L}} \operatorname{erfc}(\frac{x}{2\sqrt{Dt}} + \sqrt{\frac{t}{\tau}})] \qquad \text{(B.1a)}$$

$$F_2 = \frac{c_o L^3}{2D} (\alpha + \frac{S}{D}) e^{-\frac{t}{\tau}} [\frac{-1}{(\alpha^2 L^2 - 1)} \frac{e^{\alpha^2 L^2 \frac{t}{\tau}}}{\frac{SL}{D} + \alpha L} \cdot e^{-\alpha x}$$

$$\cdot \operatorname{erfc}(\frac{x}{2\sqrt{Dt}} - \alpha L \sqrt{\frac{t}{\tau}}) - \frac{1}{(\alpha^2 L^2 - 1)} \frac{e^{\alpha^2 L^2 \frac{t}{\tau}}}{\frac{SL}{D} - \alpha L} \cdot e^{\alpha x}$$

$$\cdot \operatorname{erfc}(\frac{x}{2\sqrt{Dt}} + \alpha L \sqrt{\frac{t}{\tau}})] \qquad \text{(B.1b)}$$

$$F_3 = \frac{c_o L^3}{2D}\left(\alpha + \frac{S}{D}\right) e^{-\frac{t}{\tau}} \left\{ -2\left(\frac{SL}{D}\right) \frac{e^{\left(\frac{SL}{D}\right)^2 \cdot \frac{t}{\tau}}}{\left\{\alpha^2 L^2 - \left(\frac{SL}{D}\right)^2\right\}\left\{\left(\frac{SL}{D}\right)^2 - 1\right\}}\right.$$

$$\left. \cdot\ e^{\left(\frac{S}{D}\right) x} \operatorname{erfc}\left(\frac{x}{2\sqrt{Dt}} + \frac{SL}{D}\sqrt{\frac{t}{\tau}}\right)\right\} \qquad \text{(B.1c)}$$

and

$$F_4 = \frac{c_o \tau}{1 - \alpha^2 L^2}\left[1 - e^{(\alpha^2 L^2 - 1)\frac{t}{\tau}}\right] \cdot e^{-\alpha x} . \qquad \text{(B.1d)}$$

By integrating each of the above equations and adding the results, Eq. (3.9) may be written as

$$C(t) = \int F_1 dx + \int F_2 dx + \int F_3 dx + \int F_4 dx .$$

For example, from Eq. (B.1a)

$$\int F_1 dx = \frac{c_o L^3}{2D}\left(\alpha + \frac{S}{D}\right) e^{-\frac{t}{\tau}} \left[\frac{1}{(\alpha^2 L^2 - 1)} \cdot \frac{e^{\frac{t}{\tau}}}{\left(\frac{SL}{D} + 1\right)}\right.$$

$$\cdot \int_o^{\ell} e^{-\frac{x}{L}} \operatorname{erfc}\left(\frac{x}{2\sqrt{Dt}} - \sqrt{\frac{t}{\tau}}\right) dx + \frac{1}{(\alpha^2 L^2 - 1)} \cdot \frac{1}{\left(\frac{SL}{D} - 1\right)}$$

$$\left. \cdot\ e^{\frac{t}{\tau}} \int_o^{\ell} e^{\frac{x}{L}} \operatorname{erfc}\left(\frac{x}{2\sqrt{Dt}} + \sqrt{\frac{t}{\tau}}\right) dx\right] \qquad \text{(B.2)}$$

which simplifies to:

$$\int F_1 dx = \frac{c_o L^3(\alpha + \frac{S}{D})}{2D(\alpha^2 L^2 - 1)} e^{-\frac{t}{\tau}} \left[\frac{1}{(\frac{SL}{D} + 1)} e^{\frac{t}{\tau}} \int_o^{\ell} e^{-\frac{x}{L}} \right.$$

$$\cdot \operatorname{erfc}\left(\frac{x}{2\sqrt{Dt}} - \sqrt{\frac{t}{\tau}}\right) dx + \frac{1}{(\frac{SL}{D} - 1)} e^{\frac{t}{\tau}} \int_o^{\ell} e^{\frac{x}{L}}$$

$$\left. \cdot \operatorname{erfc}\left(\frac{x}{2\sqrt{Dt}} + \sqrt{\frac{t}{\tau}}\right) dx \right] \qquad (B.3)$$

Several useful mathematical properties [7] are used in this process:

1) $\operatorname{erfc}(y) = 1 - \operatorname{erf}(y) = 1 - \frac{2}{\sqrt{\pi}} \int_o^y e^{-w^2} dw$

2) If $y(t) = \int_o^{f(t)} e^{-w^2} dw$ (B.4)

then $y'(t) \Rightarrow e^{-[f(t)]^2} \cdot f'(t)$.

Therefore,

$$\frac{d[\operatorname{erfc}(y)]}{dy} = \frac{-2}{\sqrt{\pi}} e^{-y^2} \cdot 1 .$$

From Eq. (B.3), using integration by parts, let

$$\operatorname{erfc}\left(\frac{x}{2\sqrt{Dt}} - \sqrt{\frac{t}{\tau}}\right) = u$$

and

$$e^{-\frac{x}{L}}\,dx = dv\ . \qquad (B.5)$$

Then

$$\frac{-2}{\sqrt{\pi}}\, e^{-\left(\frac{x}{2\sqrt{Dt}} - \sqrt{\frac{t}{\tau}}\right)^2} \cdot \frac{1}{2\sqrt{Dt}} = du$$

$$-Le^{-\frac{x}{L}} = v\ .$$

By substituting into Eq. (B.3) and simplifying, the following is obtained

$$\int F_1 dx = \frac{c_o L^3(\alpha + \frac{S}{D})}{2D(\alpha^2 L^2 - 1)}\, e^{-\frac{t}{\tau}} \Big[\frac{1}{(\frac{SL}{D} + 1)}\, e^{\frac{t}{\tau}} \Big(-Le^{-\frac{\ell}{L}}$$

$$\cdot\ \mathrm{erfc}\Big(\frac{\ell}{2\sqrt{Dt}} - \sqrt{\frac{t}{\tau}}\Big) + L\ \mathrm{erfc}\Big(-\sqrt{\frac{t}{\tau}}\Big)$$

$$- \frac{L}{\sqrt{Dt\pi}} \int_o^{\ell} e^{-\left(\frac{x^2}{4Dt} + \frac{t}{\tau}\right)} dx\Big)$$

$$+ \frac{1}{(\frac{SL}{D} - 1)}\, e^{\frac{t}{\tau}} \cdot \Big(L\, e^{\frac{\ell}{L}}\ \mathrm{erfc}\Big(\frac{\ell}{2\sqrt{Dt}} + \sqrt{\frac{t}{\tau}}\Big)$$

$$- L\ \mathrm{erfc}\Big(\sqrt{\frac{t}{\tau}}\Big) + \frac{L}{\sqrt{Dt\pi}} \int_o^{\ell} e^{-\left(\frac{x^2}{4Dt} + \frac{t}{\tau}\right)} dx\Big)\Big]\ .$$

$$(B.6)$$

In order to approximate Eq. (B.6) it is assumed that the following terms in Eqs. (B.7) and (B.8) can be neglected. These are considered as part of the constant term associated with Eq. (3.9). This assumption is verified in Section 3.3.

$$- L e^{-\frac{\ell}{L}} \operatorname{erfc}\left(\frac{\ell}{2\sqrt{Dt}} - \sqrt{\frac{t}{\tau}}\right) ,$$

$$L e^{\frac{\ell}{L}} \operatorname{erfc}\left(\frac{\ell}{2\sqrt{Dt}} + \sqrt{\frac{t}{\tau}}\right) \tag{B.7}$$

and

$$\frac{-L}{\sqrt{Dt\pi}} \int_{o}^{\ell} e^{-\left(\frac{x^2}{4Dt} + \frac{t}{\tau}\right)} dx ,$$

$$\frac{L}{\sqrt{Dt\pi}} \int_{o}^{\ell} e^{-\left(\frac{x^2}{4Dt} + \frac{t}{\tau}\right)} dx . \tag{B.8}$$

Then Eq. (B.6) may be approximated to

$$\int F_1 dx \approx \frac{c_o \tau L\left(L\alpha + \frac{SL}{D}\right) e^{-\frac{t}{\tau}} \left(\frac{-SL}{D}\right) e^{\frac{t}{\tau}} \operatorname{erfc}\left(\sqrt{\frac{t}{\tau}}\right)}{(\alpha^2 L^2 - 1)\left(\frac{SL}{D} + 1\right)\left(\frac{SL}{D} - 1\right)} . \tag{B.9}$$

Multiplying top and bottom by $-[\alpha^2 L^2 - (\frac{SL}{D})^2]$ and simplifying to

$$\int F_1 dx \approx \frac{c_o \tau L e^{-\frac{t}{\tau}}}{(\alpha^2 L^2 - 1)[(\frac{SL}{D})^2 - 1][(\frac{SL}{D}) - \alpha L]} \cdot \{[\alpha^2 L^2 - (\frac{SL}{D})^2]$$

$$\cdot (\frac{SL}{D}) e^{\frac{t}{\tau}} \operatorname{erfc}(\sqrt{\frac{t}{\tau}})\} \qquad (B.10)$$

Similar approaches can be used to find $\int F_2 dx$, $\int F_3 dx$, and $\int F_4 dx$ [Eqs. (B.1b, 1c, and 1d)] in which their sum will result in Eq. (3.9) which is similar to Eq. (2b) reported by Eranen and Blomberg [2]. Note that in all of these integrals it is necessary to make approximations similar to that of Eqs. (B.7) and (B.8). Finally, the time-dependent PCD signal, P(t), will follow the form of Eq. (A.35), except that it is no longer a function of x, as

$$P(t) = C(t)\,U(t) - C(t - t_d)\,U(t - t_d) \qquad (B.11)$$

where U(t) is a unit step function. This result is in agreement with the solution of Reference 2 [Eq. (2a)].

APPENDIX C

C.1 NEGATIVE RATIO OF THE SLOPES OF THE PCD SIGNAL

The negative ratio of the slopes (decay/increase) of the PCD signal, Eq. (4.1) is given as:

$$m = - \frac{\left.\frac{dP}{dt}\right|_{t > t_d}}{\left.\frac{dP}{dt}\right|_{0 < t < t_d}} \qquad \text{(C-1)}$$

where the time-dependent PCD signal, Eq. (3.8), is given as

$$P(t) = C(t)U(t) - C(t-t_d)U(t-t_d) \qquad \text{(C-2)}$$

and $U(t)$ is a unit step function.

Then, for $t > t_d$

$$P(t) = C(t) - C(t-t_d) \qquad \text{(C-3)}$$

and

$$\frac{dP}{dt} = C'(t) - C'(t-t_d) \qquad \text{(C-4)}$$

or

$$\left.\frac{dP}{dt}\right|_{t = t_d^+} = C'(t_d) - C'(0) \qquad \text{(C-5)}$$

where "$C'(t)$" denotes $\frac{dC}{dt}$.

Also, for $0 < t < t_d$

$$P(t) = C(t) - 0 \tag{C-6}$$

and

$$\frac{dP}{dt} = C'(t) \tag{C-7}$$

or

$$\left.\frac{dP}{dt}\right|_{t = t_d^-} = C'(t_d) \ . \tag{C-8}$$

Finally, substituting Eqs. (C-5) and (C-8) into (C-1) and simplifying,

$$m = \frac{\left.\frac{dC}{dt}\right|_{t = 0}}{\left.\frac{dC}{dt}\right|_{t = t_d}} - 1 \ . \tag{C-9}$$

From Eq. (3.9), $\frac{dC}{dt}$ can be written as

$$\frac{dC}{dt} = \frac{c_o L e^{-t/\tau}}{(\alpha^2 L^2 - 1)[(\frac{SL}{D})^2 - 1][(\frac{SL}{D}) - \alpha L]} \{-[(\alpha^2 L^2 - (\frac{SL}{D})^2]$$

$$\cdot (\frac{SL}{D}) \frac{\tau}{\sqrt{t\tau\pi}} + [(\frac{SL}{D})^2 - 1] \frac{S}{\alpha D} [e^{\alpha^2 L^2 t/\tau}$$

$$\cdot \operatorname{erfc}(\alpha L \sqrt{\frac{t}{\tau}})] (\alpha^2 L^2 - 1) - [(\frac{SL}{D})^2 - 1] \frac{S}{\alpha D} \frac{\tau \alpha L}{\sqrt{t\tau\pi}}$$

$$+ (\alpha^2 L^2 - 1) e^{(\frac{SL}{D})^2 t/\tau} \cdot \operatorname{erfc} (\frac{SL}{D} \sqrt{\frac{t}{\tau}}) \cdot [1 - (\frac{SL}{D})^2]$$

$$+ (\alpha^2 L^2 - 1) \frac{SL}{D} \cdot \frac{\tau}{\sqrt{t\tau\pi}}\} \quad . \qquad \text{(C-10)}$$

Some of the useful properties in achieving Eq. (C-10) are:

1. $L = (D\tau)^{1/2}$

2. $\operatorname{erf}(x) = \frac{2}{\sqrt{\pi}} \int_o^x e^{-\omega^2} d\omega$

3. $\operatorname{erfc}(x) = 1 - \operatorname{erf}(x)$ (C-11)

4. If $Y(t) = \int_o^{f(t)} e^{-\omega^2} d\omega$

   Then, $\frac{dY}{dt} = e^{-[f(t)]^2} \cdot \frac{df}{dt}$

5. $\frac{d}{dx} (e^u) = e^u \frac{du}{dx}$.

Factoring out the common terms in Eq. (C-10) and simplifying, results in

$$\frac{dC}{dt} = \frac{c_o L e^{-\frac{t}{\tau}}}{[(\frac{SL}{D})-\alpha L]} \{\frac{S}{\alpha D} e^{\alpha^2 L^2 \frac{t}{\tau}} \operatorname{erfc}(\alpha L \sqrt{\frac{t}{\tau}})$$

$$- e^{(SL/D)^2 \frac{t}{\tau}} \operatorname{erfc}(\frac{SL}{D} \sqrt{\frac{t}{\tau}})\} \quad . \qquad \text{(C-12)}$$

C.2 THE COMPUTER SIMULATION

A plot of the PCD signal versus the surface recombination velocity for various values of the minority carrier lifetime for an n-type GaAs sample is shown in Figure (C.1). Similar plots are shown in Figures (C.2) and (C.3) for various values of the absorption coefficients, α, for InP and GaAs, respectively.

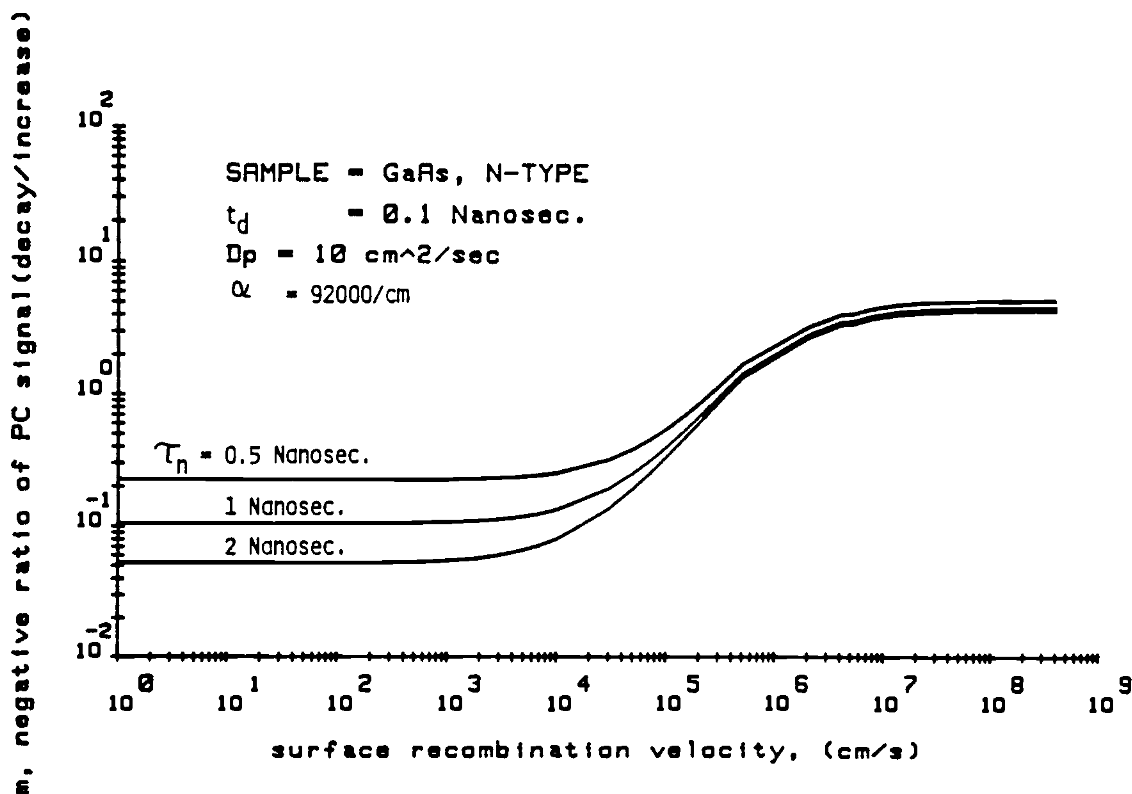

Figure C.1. A comparison of the actual surface recombination velocity for various values of the excess minority carrier lifetime.

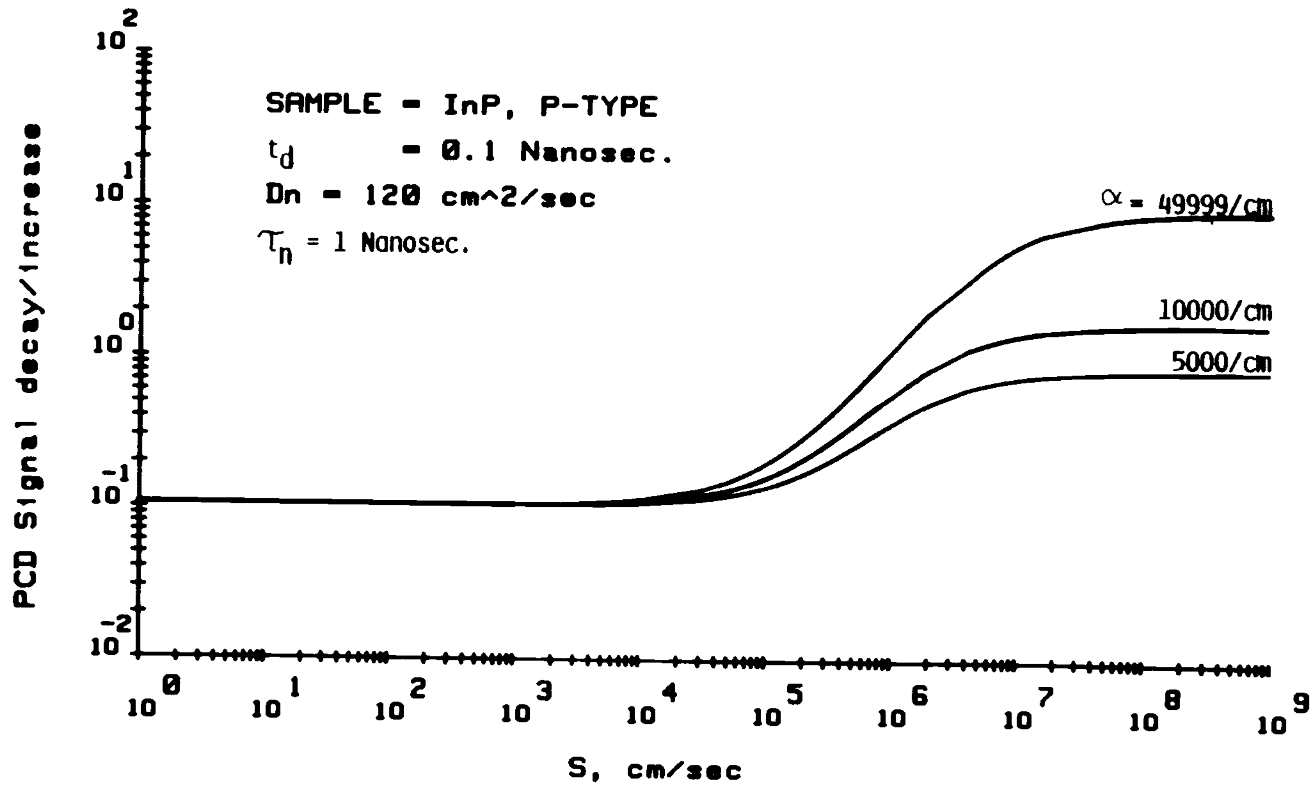

Figure C.2. Surface recombination velocity, S, for various values of Alpha.

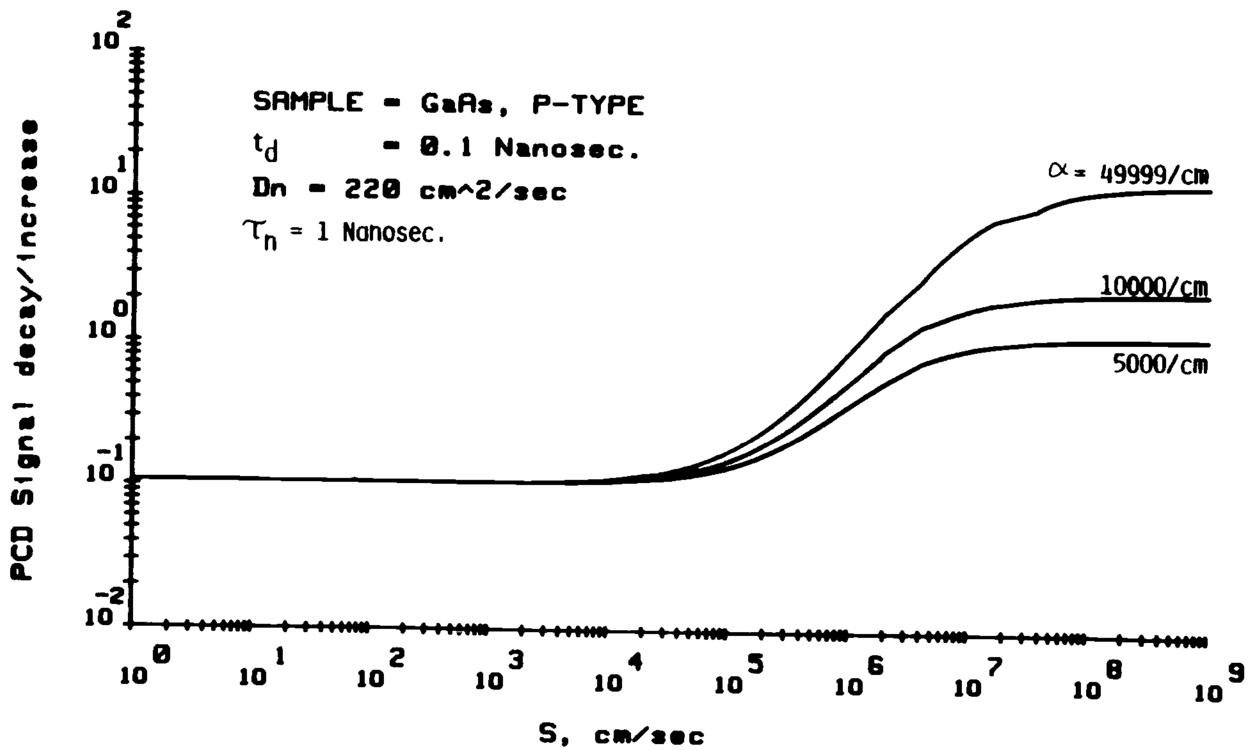

Figure C.3. Negative ratio of photoconductivity signal (decay/increase versus surface recombination velocity for various values of Alpha.

A comparison of the actual surface recombination velocity for various values of the excess minority carrier lifetime for n-type and p-type GaAs at different minority carrier doping concentrations are shown in Figures (C.4) and (C.5), respectively.

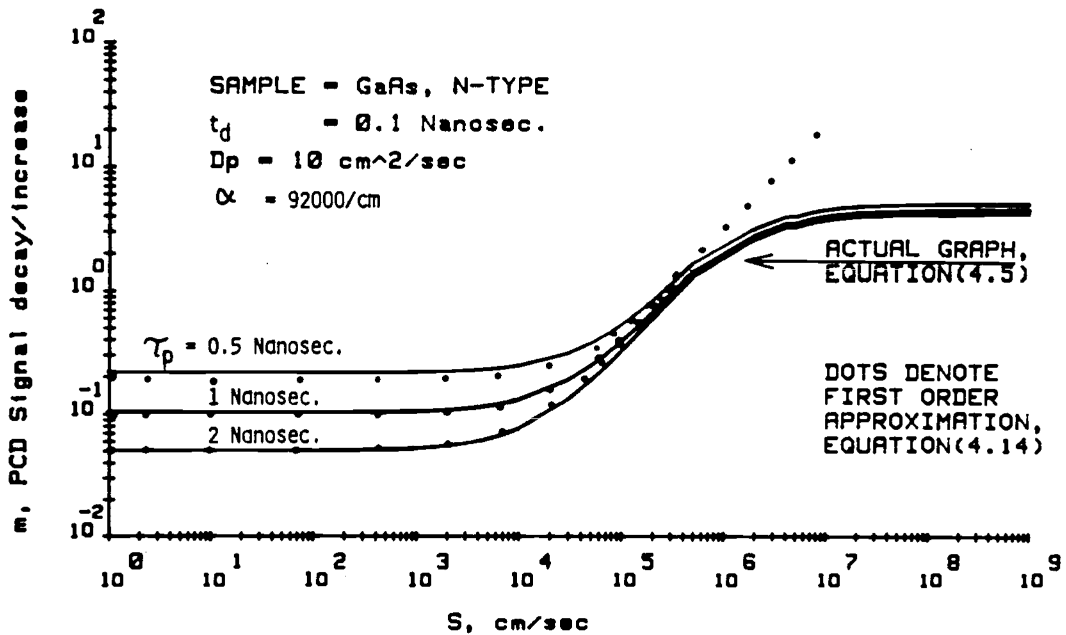

Figure C.4. A plot of the first order approximation model against the actual variation of the surface recombination velocity, S.

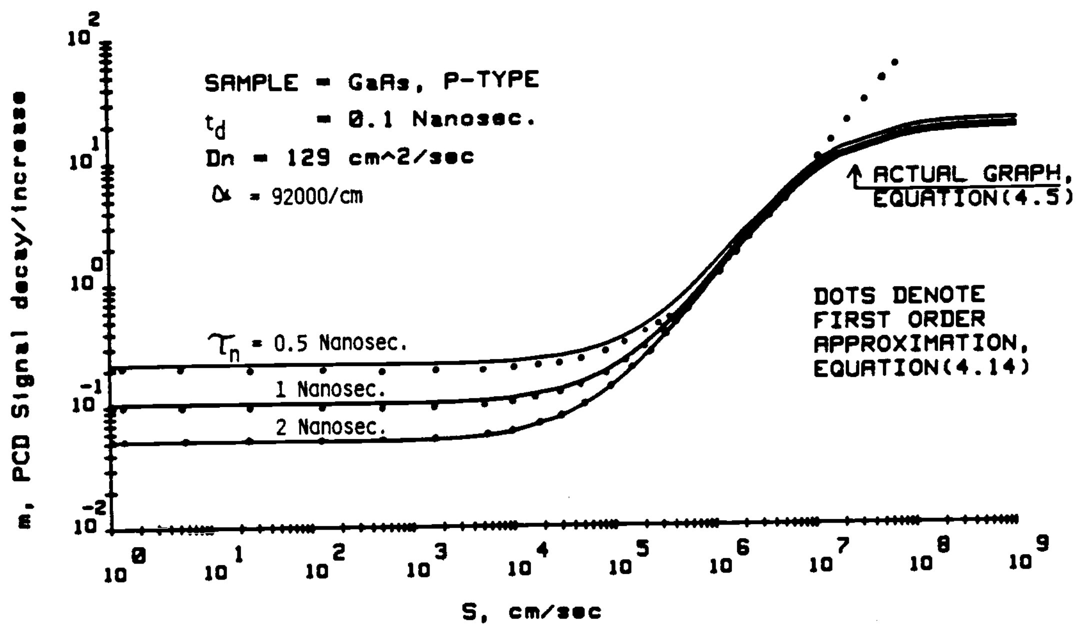

Figure C.5. A comparison of the actual variation of the surface recombination velocity and the first order approximation model.

C.3 THE FIRST ORDER APPROXIMATION

Equation (4.5) may be approximated to first order using a Taylor polynomial [10] approximation method. Let

$$m(S) = a_o + a_1 S \tag{C-13}$$

where, from Eq. (4.5),

$$a_o = m(0) = e^{\frac{t_d}{\tau}} - 1 \approx \frac{t_d}{\tau} \,, \qquad \left(\frac{t_d}{\tau} << 1\right) . \tag{C-14}$$

Note that

$$e^x \approx 1 + x \qquad \text{for } x << 1 \tag{C-15}$$

and

$$a_1 = \left.\frac{dm}{dS}\right|_{S = 0}$$

$$= -\frac{1}{\alpha D} e^{\frac{t_d}{\tau}} + e^{\frac{t_d}{\tau}} \left[\frac{1}{\alpha D} e^{\alpha^2 L^2 \frac{t_d}{\tau}} \operatorname{erfc}\left(\alpha L \sqrt{\frac{t_d}{\tau}}\right)\right.$$

$$\left. + \frac{2L}{D} \sqrt{\frac{t_d}{\tau \pi}}\right] . \tag{C-16}$$

For very large values of α, $\operatorname{erfc}\left(\alpha L \sqrt{\frac{t_d}{\tau}}\right) \approx 0$.

Note that

$$\operatorname{erfc}(\infty) = 0 . \tag{C-17}$$

Therefore, Eq. (C-16) reduces to

$$a_1 = -\frac{1}{\alpha D} e^{\frac{t_d}{\tau}} + e^{\frac{t_d}{\tau}} \left(\frac{2L}{D} \sqrt{\frac{t_d}{\tau\pi}}\right) . \qquad \text{(C-18)}$$

Using the property given in Eq. (C-15), it can be written that

$$a_1 \approx -\frac{1}{\alpha D} \left(1+\frac{t_d}{\tau}\right) + \left(1+\frac{t_d}{\tau}\right)\left(\frac{2L}{D} \sqrt{\frac{t_d}{\tau\pi}}\right) , \quad \left(\frac{t_d}{\tau} << 1\right) \qquad \text{(C-19)}$$

multiplying through and simplifying, using $L = (D\tau)^{1/2}$,

$$a_1 \approx 2 \sqrt{\frac{t_d}{D\pi}} . \qquad \text{(C-20)}$$

Substituting Eqs. (C-14) and (C-20) into Eq. (C-13), the first order approximation is

$$m(S) \approx 2 \sqrt{\frac{t_d}{D\pi}} \cdot S + \frac{t_d}{\tau} . \qquad \text{(C-21)}$$